SIRT6 OVEREXPRESSION PROTECTS AGAINST DIET-INDUCED DIABETES IN MICE

APPROVED BY SUPERVISORY COMMITTEE

Roberto Coppari, Ph.D.

Joel Elmquist, D.V.M., Ph.D.

Philipp Scherer, Ph.D.

Carol Elias, Ph.D.

Makoto Kuro-O, Ph.D.

DEDICATION

I would like to dedicate this work to my mother and father who have been pillars of love and support throughout my life.

ACKNOWLEDGEMENT

I would like to acknowledge the UTSW transgenic core facility for their help with microinjection for the generation of Sirt6BAC mice. I would also like to acknowledge Eric Berglund for his help with the hyperinsulinemic/euglycemic clamp procedure. I would also like to also acknowledge Raul Mostoslavsky for providing me with the *Sirt6* knockout mouse line.

SIRT6 OVEREXPRESSION PROTECTS AGAINST DIET-INDUCED DIABETES IN MICE

by

JASON GRAHAM ANDERSON

DISSERTATION

Presented to the Faculty of the Graduate School of Biomedical Sciences

The University of Texas Southwestern Medical Center at Dallas

In Partial Fulfillment of the Requirements

For the Degree of

DOCTOR OF PHILOSOPHY

The University of Texas Southwestern Medical Center

Dallas, Texas

August, 2013

ABSTRACT

Numerous studies in a variety of species indicate that caloric restriction (CR) elicits beneficial metabolic effects including reduced adiposity and improved glucose homeostasis, as well as enhanced insulin and leptin sensitivity. Conversely, chronic feeding on high caloric diets brings about opposite outcomes and can progress to type-II-diabetes and obesity. An intense effort by many researchers has begun to elucidate the homeostatic mechanisms accounting for these beneficial metabolic effects of CR in order to facilitate development of CR-mimetic drugs to combat the alarming increase of these diseases. Mounting experimental evidence suggests that Sirtuins may be principal mediators of the metabolic effects of CR (1). Sirtuins are believed to sense and respond to cellular energy deficit via their (NAD^+)-dependent enzymatic activities including lysine deacetylation of a variety of cytosolic, mitochondrial and nuclear proteins (2). Initial studies involving SIRT6, one of three nuclear sirtuins, suggest that it may be an attractive drug target for obesity and type-II-diabetes therapy. Knockout studies indicate that SIRT6 is required for normal growth, adiposity, and glucose homeostasis (3). Yet, contrasting these *Sirt6*-null phenotypes with those from opposing SIRT6 gain-of-function animal models lead to incongruous and seemingly contradictory conclusions regarding the stress-responsive homeostatic functions of SIRT6, casting doubt as to whether SIRT6 agonist or antagonist drugs should be sought after. To address these issues, I generated genetically engineered mice (Sirt6BAC mice) designed to eutopically overexpress SIRT6 and mimic its moderate eutopic upregulation observed during CR. This was achieved via BAC-mediated genomic insertion of an isogenic 187kb DNA region from chromosome 10 of *mus musculus* encompassing *Sirt6.* These Sirt6BAC mutants fed a high caloric diet exhibit improved glucose homeostasis as indicated via intraperitoneal glucose tolerance tests and intraperitoneal pyruvate tolerance tests. Hyperinsulinemic/euglycemic clamp indicate that these mutants exhibit enhanced insulin-sensitive inhibition of endogenous glucose production as well as enhanced blood glucose disposal and uptake into gastrocnemius and soleus muscle. Importantly, these data suggest that SIRT6 agonist drugs may be worthy of translational research for the treatment of type-II diabetes in humans.

TABLE OF CONTENTS

PRIOR PUBLICATIONS

Ramadori G, Fujikawa T, **Anderson J**, Berglund ED, Frazao R, Michán S, Vianna CR, Sinclair DA, Elias CF, Coppari R. SIRT1 deacetylase in SF1 neurons protects against metabolic imbalance. Cell Met. 2011 Sep 7;14(3):301-12.

Ramadori G, Fujikawa T, Fukuda M, **Anderson J**, Morgan DA, Mostoslavsky R, Stuart RC, Perello M, Vianna CR, Nillni EA, Rahmouni K, Coppari R. SIRT1 deacetylase in POMC neurons is required for homeostatic defenses against diet-induced obesity. Cell Metab. 2010 Jul 4;12(1):78-87.

Xu Y, Jones JE, Lauzon DA, **Anderson JG**, Balthasar N, Heisler LK, Zinn AR, Lowell BB, Elmquist JK. A serotonin and melanocortin circuit mediates D-fenfluramine anorexia. J Neurosci. 2010 Nov 3;30(44):14630-4.

Sakata I, Nakano Y, Osborne-Lawrence S, Rovinsky SA, Lee CE, Perello M, **Anderson JG**, Coppari R, Xiao G, Lowell BB, Elmquist JK, Zigman JM. Characterization of a novel ghrelin cell reporter mouse Regulatory Peptides 2009; 155(1-3):91-8.

Ramadori G, Lee CE, Bookout AL, Lee S, Williams KW, **Anderson JG**, Elmquist JK, Coppari R. Brain SIRT1: Anatomical distribution and regulation by energy availability. Journal of Neuroscience 2008; 28(40):9989-9996.

Xu Y, Jones JE, Kohno D, Williams KW, Lee CE, Choi MJ, **Anderson JG**, Heisler LK, Zigman JM, Lowell BB, and Elmquist JK. 5-HT_{2C}Rs expressed by pro-opiomelanocortin neurons regulate energy homeostasis. Neuron 2008; 60(4):582-589.

Lutter M, Sakata I, Osborne-Lawrence S, Rovinsky SA, **Anderson JG**, Jung S, Birnbaum S, Yanagisawa M, Elmquist JK, Nestler EJ, Zigman JM. The orexigenic hormone ghrelin defends against depressive symptoms of chronic stress. Nature Neuroscience 2008; 11(7):752-3.

LIST OF FIGURES

LIST OF TABLES

LIST OF ABBREVIATIONS

AMPK, AMP-activated protein kinase

BAC, Bacterial artificial chromosome

BAT, Interscapular brown adipose tissue

CR, Caloric restriction

FOXO1, forkhead box protein O1

FOXO3a, forkhead box protein O3a

HCD, High caloric diet

HGP, Hepatic glucose production

HIEC, Hyperinsulinemic-euglycemic clamp

HIF-1α, Hypoxia-inducible factor-1α

IGF, Insulin-like growth factor

IIS, Insulin/IGF intracellular signaling

IPGTT, Intraperitoneal glucose tolerance test

IPPTT, Intraperitoneal pyruvate tolerance test

InsR, Insulin receptor

NAD^+, Nicotinamide adenine dinucleotide

PGC-1α, peroxisome proliferator-activated receptor gamma coactivator 1-alpha

PPARγ, peroxisome proliferator-activated receptor gamma

Sirt6BAC, BAC-mediated SIRT6 overexpression model generated and used in this study

Sirt6-tg, CMV/βActin-driven SIRT6 overexpression model employed previously by Kanfi *et al.* (4, 5)

T2DM, Type-II diabetes mellitus

WAT, White adipose tissue

CHAPTER ONE:

Introduction

1.1 Metabolic Syndrome and Type 2 Diabetes Mellitus

Metabolic syndrome comprises a set of metabolic disorders that increase risk of developing cardiovascular disease, stroke and type 2-diabetes mellitus (T2DM) including: central/abdominal obesity, atherogenic dyslipidemia, elevated blood pressure, insulin resistance/glucose intolerance. There are several definitions that vary slightly, but in 2004, the National Cholesterol Education Program's Adult Treatment Panel III (NCEP/ATPIII) (6) declared that metabolic syndrome can be diagnosed if any three of the following risk factors are present in the patient: elevated waist circumference (≥ 102 cm for males, ≥ 88 cm for females), elevated triglyceridemia (≥150 mg/dL), decreased HDL-cholesterol (<40mg/dL for men, <50mg/dL for women), elevated fasting glycemia (≥110mg/dL), and elevated blood pressure (≥130/≥85 mm Hg).

Type 2 diabetes mellitus (T2DM) is a metabolic disorder characterized by elevated blood glucose due to insulin resistance and relative insulin insufficiency. In contrast to type 1 diabetes, characterized by 'absolute' insulin deficiency due to selective death of β-cells within the endocrine pancreas that produce and secrete the hormone, T2DM is characterized by 'relative' insulin insufficiency, due to inability of insulin to signal properly in peripheral tissues leading to elevated blood glucose. Patients with type 1 diabetes are highly insulin-sensitive, whereas prior to onset, T2DM patients undergo a period of decreasing insulin sensitivity that is compensated by an increase in the amount of secreted insulin, keeping blood glucose within the normal range. T2DM onset occurs at the stage when β-cells can no secrete enough insulin to compensate for the decreasing insulin sensitivity, resulting in impaired glucose homeostasis - a point at which patients are considered to be insulin-resistant. Whereas type 1 diabetes onset generally occurs in juveniles, T2DM was once referred to as 'adult-onset' diabetes. However, this term is no longer used due to the alarming increase within the last few decades in the number of young children with the disease. This changing epidemiological landscape highlights the need for better

treatments for T2DM, which is placing a enormous burden, not only on the lives of the people with this disease, but also on the health care system.

There is no single cause of T2DM, but genetic factors, family history, and obesity, specifically visceral adiposity, are primary risk factors for T2DM. Although a small percentage of T2DM patients have normal body mass index, they often have high waist to hip ratio characteristic of visceral adiposity. There is also a high correlation between the rise in rates of obesity and T2DM within the past 50 years. Lifestyle and dietary interventions are generally recommended including exercise and reduction of saturated fat, trans-fat and sugar in the diet. Additionally, drugs shown to activate AMP-activated protein kinase (AMPK) such as metformin (7, 8) and thiazolidindiones(9) have proven effective and may be prescribed for the management of T2DM.

1.2 Caloric Restriction

Caloric restriction (CR), sometimes referred to as dietary restriction, is a dietary regimen consisting of 30-40% fewer calories than *ad-libitum* caloric intake without malnutrition. CR is the only dietary intervention that has been consistently shown to extend lifespan in all organisms studied to date. In addition to its well-publicized lifespan-extending effect, CR also delays the onset of multiple age-associated diseases including cancer, neurodegenerative disease and diabetes in several species, including *Saccharomyces cerevisiae* (budding yeast), *Caenorhabditis elegans* (nematode worm), *Drosophila melanogaster* (fruit fly), *Danio rerio* (zebrafish), rodents, *Macaca mulatta* (rhesus macaque) and possibly humans (10-18).

The vast majority of studies regarding CR have focused on its purported effect on longevity *per se*. While it is not the goal of this work to focus on the lifespan extending aspect of CR, it would be remiss to neglect it. Varying degrees of lifespan extension have been observed in every species studied ranging from budding yeast to rhesus macaques (19). Disparate studies involving mutations in various components of two evolutionarily conserved nutrient-signaling pathways have been shown to extend lifespan: the insulin/ insulin-like growth factor signaling (IIS) pathway (20-24) and the target of

rapamycin (TOR) intracellular signaling pathway (25-33). Interestingly, both are nutrient-sensing and growth signaling mechanisms. This point is interesting to note, because certain gene mutations that may enhance replicative lifespan (measured in cell divisions prior to senecence) negatively impact chronological lifespan (measured in survival time of nondividing cells) (34). Sirtuins have also been suggested to prolong lifespan, which is discussed subsequently (5, 35-37).

Two prominent longitudinal studies investigating effects of CR on longevity and health and disease in rhesus macaques were conducted at the Wisconsin National Primate Research Center (WNPRC) and the National Institute on Aging (NIA) (14, 16). These two studies generated much publicity due to their rarity stemming from the long timeframe (25 years) necessary to conduct such studies in a long-lived primate species and because Rhesus monkeys are the most closely related model organism to humans. The basic premise of these studies was simple: a CR experimental group of monkeys would be fed roughly 30% less than the control group, and basic health parameters would be measured. The WNPRC study, which began in 1989, concluded that CR extended life span, as 13% of the CR monkeys died of age-related causes compared with 37% from the control group during the study timeframe. Surprisingly, the NIA study, which began in 1987, showed no such effect on mean lifespan. Although the two studies were conducted in parallel and intended to be as similar as possible, several differences may have accounted for the discrepant conclusions regarding lifespan. The NIA monkeys were fed meals that included fish oil and antioxidants, whereas the WNPRC diet did not; and WNPRC diet contained 28.5% sucrose, whereas the NIA diet contained just 3.9% sucrose. Additionally, the WNPRC control group likely ate more than the NIA control group because they were fed *ad libitum* versus the fixed amounts the NIA monkeys were fed, which may have accounted for the WNPRC control monkeys weighing more than the NIA control monkeys as adults (though the NIA monkeys descended from genetic lines from India and China, whereas the WNPRC monkeys all came from India). If these differences in diet composition constituted a more unhealthy diet for WNPRC monkeys, then their CR monkeys may have appeared healthier in comparison because they ate less of it. The implication here is that the WNPRC observations reflected an unhealthy control group rather than a long-lived treatment

group. As it currently stands, it is difficult to conclude whether CR has a beneficial effect on longevity *per se* or not.

While being less-publicized than the potential lifespan extending effects of CR, there is more consensus regarding the evidence in support of the metabolic health benefits of CR in mammals (13, 14, 16, 18, 25, 38, 39). In mice, these benefits include lower insulin levels, enhanced insulin sensitivity, reduced triglycerides, blood pressure, arterial stiffness and cholesterol, and elevated HDL. Indeed these effects are consistent with the results obtained in the NIA and WNPRC studies with rhesus macaques; significant reductions in body weight, triglycerides, cholesterol and glycemia were observed in the CR group compared with their respective controls. Additionally, CR delayed the onset of age-related diseases including cancer, diabetes and neurodegenerative disease as well as cardiovascular disease in the WNPRC study but not in the NIA study.

Regrettably, the precise mechanisms underlying these beneficial effects of CR on metabolic parameters remain poorly understood. Therefore, critically investigating these mechanisms through hypothesis-driven scientific experimentation will help to elucidate the critical molecular targets for effective therapies (CR mimetics) for diet-induced obesity and/or T2DM.

1.3 Sirtuins

Sirtuins are evolutionarily conserved nicotinamide adenine dinucleotide (NAD^+)-dependent enzymes mediating posttranslational modifications on a variety of cytosolic, nuclear and mitochondrial proteins. NAD^+ is an ancient and fundamental coenzyme produced by all cells and plays a critical role in redox reactions with its ability to transition between the oxidized form NAD^+, and the reduced form NADH. Sirtuins are classic metabolic sensor proteins, in that they sensitive to the metabolic state of the cell due to their enzymatic dependency on available NAD^+. While high concentrations of NAD^+ activate Sirtuins, NADH is a competitive inhibitor of Sirtuins activity (40, 41). Therefore, the ratio of cellular NAD^+/NADH can acutely modulate the activity of Sirtuins (40-44). The ratio of NAD^+/NADH also provides a signal of the metabolic state of the cell due to its involvement in metabolic pathways. In the

energy-replete metabolic state, cellular metabolism relies primarily on glycolysis for ATP generation, with associated conversion of NAD^+ to NADH by Glyceraldehyde phosphate dehydrogenase. This drives the NAD^+/NADH ratio lower. However, during periods of energy deficit such as fasting or prolonged CR, reduced glucose availability reduces the glycolytic flux resulting in less NADH production from glycolysis. Cellular metabolism shifts towards mitochondrial aerobic respiration. Redox reactions in the TCA cycle reduce NAD^+ to NADH, which is then oxidized back to NAD^+ by NADH:ubiquinone oxidoreductase in complex I of the mitochondrial electron transport chain. This process drives the NAD^+/NADH ratio higher during periods of caloric deficiency. Indeed, the NAD^+/NADH ratio was shown to increase in muscle and white adipose tissue, and likely other tissues as well (45, 46). It is also quite possible that other enzymes, which are responsive to cellular energy status, make post-translational modifications on Sirtuins thereby affecting their activity (47). Additionally, the overall enzymatic activity performed by Sirtuins in any given cell may increase in response to caloric deficit simply via an increase in Sirtuin protein levels, a phenomena which has been observed for several Sirtuins (48-52).

In addition to its role in cellular metabolism, NAD^+ is also used in posttranslational modification reactions, where chemical groups are added or removed from proteins, notably in ADP-ribosylation and deacetylation reactions by Sirtuins. Deacetylation of lysine residues, the most well studied enzymatic function of Sirtuins, is coupled to NAD^+ hydrolysis, yielding the deacetylated protein and the byproducts O-acetyl-ADP-ribose and nicotinamide (41, 53, 54). Nicotinamide, is itself an inhibitor of Sirtuin activity (53, 55), resulting in a negative-feedback mechanism. Less commonly, some Sirtuins (SIRT4, SIRT6) exhibit mono-ADP-ribosyltransferase activity, which transfers a single ADP-ribose moiety onto an arginine, glutamate or aspartate residue. The reaction also requires NAD^+ and yields only nicotinamide.

Sirtuins' namesake, the *Saccharomyces cerevisiae* Silent information regulator-2 (SIR2), was the first Sirtuin to be discovered. As its name implies, SIR2 (Silent Information Regulator 2) in yeast is necessary for transcriptional silencing at hidden mating-type loci (56, 57), telomeres (58) and rDNA (59). A large amount of publicity was generated following published observations of 30% replicative lifespan extension via integration of a second copy of Sir2 into the yeast genome. Conversely, Sir2 deletion was

reported to reduce the replicative lifespan of yeast by approximately 50% (37). This effect on lifespan was postulated to occur by affecting the rate of extrachromosomal rDNA circle formation, which has been shown to negatively affect yeast longevity (60, 61). Consistent with the hypothesis that both SIR2 and FOB1 (a rDNA replication fork barrier protein, whose deletion reduces formation of extrachromosomal rDNA circles and increases replicative lifespan by 30%–40% (62)) affect yeast lifespan through a common pathway regulating extrachromosomal rDNA circle formation, overexpression of SIR2 in the context of FOB1 deletion does not extend lifespan (37). Additionally, several reports suggest that the lifespan extending effects of CR are SIR2 activity-dependent (42, 44, 63-65). However, this hypothesis has been met with a large amount of skepticism (66-70), as several pieces of experimental evidence suggests that the lifespan extending effects of CR and SIR2 occur through exclusive parallel mechanisms (69, 70) and/or appear due to artifacts arising from the genetic background in these models (71).

Regardless of whether SIR2 may or may not promote lifespan extension *per se*, reproducible observations indicate that Sirtuins in more complex multicellular organisms orchestrate diverse homeostatic responses to various types of cellular stress. Sirtuin homologs within multicellular organisms with specialized organ systems likely evolved additional complexity with multifaceted and nuanced functions. These multifaceted functions at the cellular level and organ level would have evolved because they ultimately helped to promote homeostasis at the level of the organism. Thus, although it remains unclear whether Sirtuins govern lifespan *per se*, the cumulative effect of these homeostatic responses are likely to provide protection against various types of cellular stress, which may indirectly protect against disease and premature death. This rationale led me to study Sirtuins in more specific homeostatic roles and in the context of metabolic disease states in a mammalian model organism, *Mus musculus*.

Evolutionary divergence has produced seven SIR2 homologues in mammalian species (SIRT1-SIRT7) with different enzymatic, metabolic and homeostatic functions and substrate specificity depending on cell-type and subcellular localization. SIRT2 is predominantly cytosolic, while SIRT3, SIRT4 and SIRT5 reside in the mitochondria. Of particular interest are the nuclear-localized Sirtuins (SIRT1, SIRT6, and SIRT7), which have the unique ability to deacetylate certain lysine residues on

histone proteins in addition to non-histone proteins. Histones are the fundamental components of chromatin that package roughly two meters of human genomic DNA into the nucleus of each human cell. Lysine residues are positively charged and have high affinity for the negatively charged phosphate deoxyribose backbone of DNA, resulting in a tightly bound DNA-chromatin quaternary structure that renders the DNA sequence inaccessible to accessory factors due to stearic hindrance. When these lysine residues are acetylated via the actions of histone acetyltransferases, the positive charge is neutralized, resulting in a more loosely bound structure, and allowing accessory factors to interact with the double helix. Therefore, lysine-deacetylation of histones by nuclear Sirtuins leads to greater stearic hindrance of DNA-transcription factor interactions, resulting in transcriptional silencing of genes within these regions of tightly packed facultative heterochromatin. This property of SIRT1, SIRT6, and SIRT7 makes these nuclear Sirtuins particularly interesting targets for study, because it suggests that they have the ability to orchestrate cellular homeostatic mechanisms at the level of gene transcription.

The most extensively studied mammalian Sirtuin, and the orthologue of yeast SIR2, is SIRT1. SIRT1 has been shown to deacetylate lysine residues of histone proteins including H3K9, H3K14, H4K16 and H1K26 to promote formation of facultative heterochromatin and silence gene transcription (72). Additionally, SIRT1 interacts with and modulates the activity of a number of transcription factors localized at euchromatin. SIRT1 was demonstrated to deacetylate the K382 residue of p53 and inhibit its transcriptional ability, leading to suppression of p53's apoptotic effects (73). SIRT1 was also shown to deacetylate the RelA subunit of nuclear factor kappa-light-chain-enhancer of activated B cells (NF-κB) at K310 and inhibit the transcriptional activity of NF-κB (74). This inhibition also sensitized cells to TNFα-induced apoptosis. Additionally, SIRT1 has been shown to affect the activity of mTOR, the catalytic subunit of the metabolic nutrient sensor mammalian target of rapamycin protein complex-1 (mTORC1). mTORC1 is a serine/threonine protein kinase that integrates nutrient stimuli, redox stress and growth-promoting signaling pathways and regulates cell growth and proliferation by modulating transcription and translation. SIRT1 was shown to inhibit mTORC1 through its interaction with TSC2 (a component of the mTOR inhibitory-complex TSC1/TSC2) (75).

SIRT1 has also been shown to play an important role in glucose, lipid and cholesterol metabolism. SIRT1 is capable of deacetylating and activating peroxisome proliferator-activated receptor gamma coactivator 1-alpha (PGC-1α), which leads to increased hepatic gluconeogenesis, fatty acid oxidation, mitochondrial biogenesis, and oxidative phosphorylation (76-79). SIRT1 also activates the transcription factor forkhead box protein O1 (FOXO1), also resulting in increased gluconeogenesis (80). SIRT1 has also been shown to deacetylate peroxisome proliferator activated receptor gamma (PPARγ) at specific lysine residues necessary to recruit the brown adipose tissue (BAT) Program coactivator PR domain containing 16 to PPARγ, leading to selective induction of BAT genes leading to "browning" of white adipose tissue (81). Knockdown of SIRT1 in livers of fasted mice reduces expression of fatty acid β-oxidation genes (82). Additionally, two distinct liver-specific *Sirt1*-knockout models display decreased fatty acid β-oxidation, fatty liver, hepatic steatosis, inflammation and endoplasmic reticulum stress (77, 83). SIRT1 also affects hepatic cholesterol and bile acid homeostasis through deacetylation of the nuclear hormone receptors: liver X receptor farnesoid X receptor and the sterol regulatory element binding protein family of transcription factors (77, 84-89).

Resveratrol is a plant polyphenol capable of increasing the average lifespan of *S. cerevisiae* (90) as well as *C. elegans* and *D. melanogaster* (91). Resveratrol has also been reported to protect against cardiovascular disease, cancer, age-related deterioration and the pathological metabolic effects of high-fat diet. As such, it has widely been considered a CR mimetic. Resveratrol was initially reported to elicit CR-like effects through direct activation of SIRT1 *in vitro* (90). However, this finding has come under heavy scrutiny as being an artifact of the unique assay used (92-95). A direct target of resveratrol has remained elusive until recently; Park *et al*. (96) revealed that resveratrol is a competitive inhibitor of several Phosphodiesterases. Resveratrol's inhibitory effect on Phosphodiesterases leads to a cascade of intracellular events resulting in activation of AMPK. As a consequence, resveratrol increases NAD^+ and the activity of SIRT1 in an AMPK-dependent fashion. Resveratrol was shown to improve mitochondrial function and enhance insulin sensitivity, associated with decreased acetylation and increased activity of

PGC-1α (79). Moderate doses of resveratrol were shown to increase mitochondrial biogenesis, NAD^+ levels and activate AMPK in a SIRT1-dependent manner(97). AMPK activation was also associated with increased cellular NAD^+ levels and decreased acetylation of SIRT1 targets including the transcription factors PGC-1α, FOXO1 and forkhead box protein 3a (FOXO3a) (98). SIRT1 was also shown to be required for resveratrol's ability to increase insulin sensitivity by silencing transcription of *PTP1B* (99). Collectively, these reports suggest that pharmacologically or genetically induced activation of SIRT1 can protect against derangements in glucose and lipid homeostasis caused by HCD feeding in rodents (79, 100-105).

The glaring similarities between the effects of SIRT1 activation and CR suggests that SIRT1, and likely other Sirtuins, function to mediate the homeostatic responses to the various types of cellular stress arising during periods of energy deficit. As the seven mammalian Sirtuins are likely to have complementary, but non-redundant homeostatic functions, it remains the goal of numerous investigators to dissect the specific cellular mechanisms mediated by each one. A rich coordinated interplay between Sirtuin members is likely to unfold.

1.4 SIRT6

In 2006, Mostoslavsky *et al.* reported that *Sirt6* knockout (*Sirt6*$^{-/-}$) mice display profound progeria and severe degenerative phenotypes associated with aging including lymphopenia, osteopenia, lordokyphosis, malocclusion, and colitis as well as telomere abnormalities, sensitivity to genotoxic stress, loss of subcutaneous fat, small size, low insulin-like growth factor-1 (IGF1) levels, severe hypoglycemia, and mortality around four weeks of age (3). Since Sirtuin homologues in other species were already being studied for their effects on lifespan regulation, these observations by Mostoslavsky *et al.* elicited a great deal of excitement in the field of aging research, and metabolism alike, and SIRT6 quickly became one of the most hotly investigated mammalian Sirtuins to date.

While SIRT6 still hasn't been as extensively studied as SIRT1, key insights into its function have been elucidated in recent years. Like SIRT1, SIRT6 deacetylates histone substrates including histone 3 lysine 9 (H3K9) (106) and histone 3 lysine 56 (H3K56) (107). Unlike SIRT1, SIRT6 also possesses mono-ADP-ribosyltransferase activity (108). SIRT6 is expressed in all tissues to varying degrees under basal conditions, exhibiting the highest protein levels in thymus, heart, skeletal muscle and brain (3, 51, 108). SIRT6 is also significantly upregulated within 18 hours of acute fasting in brain, white adipose tissue (WAT), and liver (51) and during CR in brain, WAT, kidney, and heart (52).

SIRT6 has been implicated in the maintenance of telomere structure. Michishita *et al.* (106) first demonstrated that loss of SIRT6 leads to abnormal telomere structure resembling defects observed in Werner syndrome (a premature ageing disease), end-to-end chromosome fusions, and premature cellular senescence. Furthermore, SIRT6 was found to specifically associate with chromatin at telomeres and deacetylate H3K9, which is required for stable association of WRN, a protein that is mutated in Werner syndrome. Subsequently, Michishita *et al.* (107) found that acetyl-H3K56 is also a specific target of SIRT6 deacetylase activity and showed that SIRT6 leads to dynamic acetylation states of H3K56 at telomeric chromatin throughout various stages of the cell cycle. Tennen *et al.* also demonstrated that SIRT6 is required for maintenance of the telomere position effect, which is the epigenetic silencing of genes proximal to telomeres due to a repressive heterochromatin environment, by showing that RNAi-mediated knockdown of SIRT6 abrogated the silencing of both an endogenous gene and an integrated transgene proximal to telomeres.

SIRT6 has also been shown to be involved in DNA repair (3, 109-112). Mostoslavsky *et al.* first reported that *Sirt6*-null mouse embryonic fibroblasts (MEFs) exhibit genomic instability, displaying chromosomal abnormalities including fragmented chromosomes, detached centromeres, gaps and translocations (3). Furthermore, these MEFs displayed hypersensitivity to DNA damage induced by specific genotoxic agents: methyl methanesulfonate, hydrogen peroxide, and infrared radiation, which are consistent with defects in base excision repair, but not ultraviolet radiation, which is repaired via nucleotide excision repair. This pattern of genotoxic sensitivity suggests that SIRT6 may modify certain

base excision repair factors or modulate chromatin to allow base excision repair factors to access sites of DNA damage. However to date, no interactions between SIRT6 and any base excision repair factors have been discovered. Subsequently, a report by McCord *et al.* (109) implicated SIRT6 in DNA double strand break (DSB) repair. They found that following induction of DNA DSBs, levels of acetylated H3K9 decrease in a SIRT6-dependent manner. Furthermore, SIRT6 specifically interacts with DNA-dependent protein kinase (DNA-PK), a protein involved in non-homologous end joining (NHEJ), and is required for the mobilization of catalytic subunit of DNA-PK to chromatin adjacent to induced site-specific DSBs. These data suggest that SIRT6 may function to deacetylate H3K9 surrounding DSBs, and stabilize DNA-PK and possibly other NHEJ factors at sites of DSBs to promote DSB repair. Subsequently, Kaidi *et al.* (110) reported in 2010 that SIRT6 has a role in DNA end resection, a step in DSB repair by homologous recombination (HR). They showed that the accumulation of replication protein A and the rate of HR were impaired at sites of DNA damage due to SIRT6 depletion. The DSB resection factor C-terminal binding protein interacting protein (CtIP) was identified as a SIRT6 interaction partner and was shown to be selectively deacetylated by SIRT6. A CtIP mutant protein, which cannot be acetylated, abrogated the impaired resection observed with SIRT6-depletion, suggesting that SIRT6-dependent deacetylation of CtIP promotes DNA resection. Furthermore, in 2011 Mao *et al.* (111) reported the association of SIRT6 with another DSB repair factor, poly[adenosine diphosphate-ribose] polymerase 1 (PARP1). They demonstrated that in response to oxidative stress, SIRT6 physically associates with PARP1 and is recruited to sites of DNA DSBs, where it mono-ADP-ribosylates lysine residue 521 of PARP1, activating the poly-ADP-ribosylase activity of PARP1. This activity promotes DSB repair through potentially both NHEJ and HR mechanisms under oxidative stress. It was later reported by these investigators (112) that DSB repair by HR declines with replicative age along with expression of several proteins involved in HR, including SIRT6, into cellular senescence. However, this decline in HR could be rescued with overexpression of SIRT6 in presenescent cells, and this effect was dependent upon the mono-ADP ribosylase activity of PARP1, which they previously showed to be SIRT6-dependent. All together, these data suggest that SIRT6 plays an integral role in the homeostatic response to DNA damage.

As previously stated, SIRT6 is capable of silencing gene transcription via epigenetic deacetylation of specific histone lysine residues. The gene silencing specificity of SIRT6 appears to occur through the association of SIRT6 with particular transcription factors that determine its localization on specific gene promoter regions. One of these transcriptional interaction partners is NF-κB, a transcription factor complex that mediates inflammatory and innate immune responses signaled by stress stimuli such as: various cytokines (TNFα, IL-1β, oxidative stress (ROS, ionizing radiation) and bacterial or viral infection (lipopolysaccharides, toll-like receptor signaling) (113-117). The NF-κB complex consists of five protein subunits: NF-κB1, NF-κB2, RelA, RelB, and c-Rel. The NF-κB complex is normally sequestered in an inactive state in the cytoplasm by inhibitor of κB proteins, which bind to, and mask the nuclear localization signal on NF-κB subunits (118). In response to these stress stimuli, these intracellular signaling networks lead to ubiquitination and proteosomal degradation of inhibitor of κB proteins, thereby exposing the nuclear localization signal of NF-κB, allowing it to enter nucleus and modulate the transcription of its target genes. In 2009, Kawahara *et al.* (119) reported that SIRT6 physically binds to the RelA subunit of NF-κB and is recruited to NF-κB target gene promoters. They observed hyperacetylation of H3K9 at NF-κB target promoters, increased RelA promoter occupancy, and increased NF-κB-dependent gene transcription in SIRT6-deficient cells. Furthermore, the early lethality and progeroid-like phenotypes of *Sirt6*$^{-/-}$ mice were rescued by haploinsufficiency of RelA. These data suggest that SIRT6 attenuates NF-κB target gene transcription and that the premature aging in *Sirt6*$^{-/-}$ mice is due to hyperactive NF-κB signaling. In a subsequent report, Kawahara *et al.* employed genome-wide profiling of RelA- and SIRT6- bound sites, showing that SIRT6 promoter occupancy is highly dynamic in response to treatment with TNFα – an upstream regulator of NF-κB activity. Overall, SIRT6 occupies 54% of NF-κB target promoters and 29% of SIRT6 gene targets are shared by RelA. The 1481 genes occupied by both proteins are associated with cell senescence and organismal aging. Of note, direct inhibition of NF-kB was also suggested to be induced by SIRT1(74), lending support to the idea that SIRT1 and SIRT6 have complementary, but non-redundant functions.

One of the more striking phenotypes of the *Sirt6*$^{-/-}$ mouse is its reduced size. In 2010, Schwer *et al.* (120) reported that a neural-specific SIRT6-deficient mouse model displayed low growth hormone (GH) and IGF1 levels, recapitulating the postnatal growth retardation and somatotropic attenuation of *Sirt6*$^{-/-}$ mice, suggesting that the reduced growth of *Sirt6*$^{-/-}$ mice is attributed to defects in SIRT6-signaling beginning within the central hypothalamic-pituitary axis. These mice did not display postnatal lethality and over time, reached normal size and eventually became obese. Interestingly, these phenotypes are also strikingly similar to several neuronal-specific SIRT1-deficient mouse models (102, 121, 122), lending support for the complementary, but non-redundant roles of SIRT1 and SIRT6. In 2012, Sundaresan *et al.* (123) discovered that SIRT6 attenuates IGF1-AKT intracellular signaling via silencing transcription of genes involved in this intracellular signaling pathway. They showed that deletion of *Sirt6* in adult mouse hearts (using a tamoxifen-inducible myosin heavy chain-Cre system) led to cardiac hypertrophy and eventual heart failure. They also observed significantly increased amounts of proteins belonging to the IGF-AKT signaling pathway including IGF1 receptor (IGF1R), insulin receptor (InsR), extracellular signal-regulated kinase 1 (ERK1), AKT, FOXO1, glycogen synthase kinase 3 and insulin-like growth factor-2 (IGF2) in these SIRT6-deficient hearts. Conversely, cardiac-specific SIRT6-overexpressing mice were protected from cardiac hypertrophy in response to hypertrophic stimuli. Furthermore, they showed that SIRT6 interacts with the transcription factor c-Jun and deacetylates H3K9 at c-Jun target promoters. These data suggest that SIRT6 acts to suppress cardiac hypertrophy by silencing transcription of genes belonging to the IGF-AKT signaling pathway, whereas in response to growth factors and hypoxic stress, SIRT6 may be inactivated and lead to cardiac hypertrophy. Once again, these results mirror the phenotypes of SIRT1-deficiency, as Sasone *et al.* showed that IGF1 and IGFR were negatively regulated by SIRT1 (124). Consistent with these data, Kanfi *et al.* (5) reported that ubiquitous transgenic SIRT6 overexpression leads to decreased serum IGF1 levels and altered phosphorylation of major components of the IGF-AKT signaling pathway consistent with reduced IGF-AKT signaling. Additionally, male, but not female, *Sirt6*-overexpressing mice exhibited extension of

lifespan. This is interesting, as defects in IGF signaling in other organisms have also been reported to extend lifespan (20-24).

In addition to their pronounced progeroid phenotypes and reduced growth, *Sirt6*$^{-/-}$ mice also exhibit acute onset of hypoglycemia beginning around 3 weeks of age before dying within several weeks of age. The effects of SIRT6 on glucose homeostasis were investigated in further detail by Zhong *et al.* (125). They reported that SIRT6 functions to downregulate the transcriptional activity of hypoxia-inducible factor 1-alpha (HIF-1α). HIF-1α is a transcription factor that, as its name implies, is a principal mediator of cellular adaptation to hypoxic stress (126, 127). During hypoxic conditions, cells conserve oxygen by shifting the carbon metabolic flux away from aerobic (mitochondrial) respiration. Instead cells rely on the inefficient anaerobic glycolysis pathway for ATP production and shunt pyruvate away from the mitochondria, and use the pyruvate to oxidize the NADH produced in glycolysis (generating lactate via lactate dehydrogenase) in order to replenish NAD^+ so glycolysis can continue (128, 129). HIF-1α is directly involved with this effect. During normoxic conditions, HIF-1α is hydroxylated by prolyl-hydroxylase domain proteins. This hydroxylation marks HIF-1α for subsequent proteasome degradation, but when oxygen levels fall, prolyl-hydroxylase domain proteins are inactivated, stabilizing HIF-1α (128). HIF-1α upregulates expression of genes involved in glycolysis, leading to an increase in glycolytic flux (130), which is needed due to the decreased efficiency of ATP-generation in anaerobic versus aerobic metabolism. HIF-1α also complements this activity by inhibiting mitochondrial respiration through upregulation of pyruvate dehydrogenase kinase (PDK) (131, 132), an enzyme that inactivates pyruvate dehydrogenase (PDH), which converts pyruvate to acetyl-CoA to supply the TCA cycle. Zhong *et al.* (125) demonstrate that *Sirt6*$^{-/-}$ cells exhibit increased membrane localization of glucose transporter-1 (GLUT1) and cell-autonomous glucose uptake, increased glycolysis, increased lactate production and decreased oxygen consumption. Additionally, they observed increased lysine-acetylation at H3K9 concomitant with increased HIF-1α activity at glycolytic gene promoters in *Sirt6*$^{-/-}$ cells. Lack of HIF-1α also reduced the binding of SIRT6 at these promoters suggesting that SIRT6 is recruited to these

promoters via association with HIF-1α. Furthermore, they showed that downregulation of HIF-1α abrogates the increased glucose uptake and upregulation of glycolytic genes observed in SIRT6-deficient cells. These data were largely recapitulated later in 2010, with a different *Sirt6*-knockout mouse line by Xiao *et al.* (133). They further demonstrated that SIRT6-deficiency leads to activation of AKT via upregulation of upstream proteins including InsR, insulin receptor substrate-1 (IRS1), insulin receptor substrate-2 (IRS2). This data may be suggestive of the following model: During hypoxic stress, cells will preserve oxygen at the expense of low metabolic efficiency (ATP production per glucose). During periods of caloric deficiency, cells preserve energy-containing macromolecules such as glucose at the expense of oxygen by shifting metabolic flux toward (efficient ATP production) mitochondrial oxidative phosphorylation, generating 36 molecules of ATP per molecule of glucose. In this regard, these data suggest that SIRT6 competes with HIF-1α for transcriptional activation/inactivation of glycolytic genes to counterbalance the oxygen-preserving functions of HIF-1α with the necessity for glucose preservation during caloric deficit.

Interestingly, it was also noted that the increased glycolytic capacity and reduced mitochondrial respiration observed in SIRT6-deficient cells, is reminiscent of the "Warburg effect" first described by Otto Warburg in 1956 (134). In brief, the Warburg effect describes the observation that cancerous tumors produce energy predominantly through a high rate of glycolysis followed by lactic acid fermentation, rather than efficiently oxidizing pyruvate for ATP production in mitochondria. This observation of the Warburg-like metabolic state of SIRT6-deficient cells was indeed insightful, as SIRT6 was later shown by Sebastian *et al.* to be a novel tumor suppressor (135). They found that SIRT6-deficiency led to increased aerobic glycolysis and increased tumor number, size and aggressiveness without activation of any known oncogenes. Furthermore, they identified MYC as yet another transcription factor that associates with SIRT6. They found a significantly high percentage (752 of top 1,0000 genes) of MYC target genes promoters that were also enriched for SIRT6 occupancy. These genes are involved in ribosome biosynthesis, consistent with previously described function of MYC (136). MYC expression

and protein stability were not affected by deficiency of SIRT6, nor were the acetylation levels of MYC or H3K9. However, a significant increase in H3K56 acetylation was found on these promoter regions. These data suggest that SIRT6 interacts with MYC on the promoters of genes involved in ribosome biosynthesis and corepresses MYC transcriptional activity by deacetylating H3K56.

Liver metabolism plays a central role in whole body glucose homeostasis. Hepatic glucose production (HGP) comprises two mechanisms of supplying glucose to the blood circulation: glycogenolysis and gluconeogenesis. The liver releases glucose from the glucose-storage molecule, glycogen (glycogenolysis) in response to activation of the sympathetic arm of the autonomic nervous system, which leads to direct norepinephrine release from sympathetic postganglionic neurons and epinephrine release from the adrenal medulla. During hypoglycemia, the liver responds to decreasing insulin and increasing glucagon in blood by activating *de novo* glucose synthesis (gluconeogenesis) from several non-carbohydrate carbon substrates such as lactate, glucogenic amino acids, and the products of triglyceride lipolysis, which enter the gluconeogenic pathway through their metabolism to pyruvate, oxaloacetate, or glycerol. Given the importance of the liver and the pronounced effects that SIRT6 have on glucose homeostasis, Kim *et al.* (51) investigated the role of SIRT6 in the liver with a hepatocyte-specific *Sirt6*-knockout mouse model. Deletion of *Sirt6* in the liver led to aberrant gene expression, increased glycolysis, increased triglyceride synthesis and reduced beta-oxidation resulting in fatty liver at 5-6 months of age. They found increased expression of genes involved in glycolysis: glucokinase (*Gk)*, liver pyruvate kinase (*Lpk*), and triglyceride synthesis: acetyl-CoA carboxylase-1 (*Acc1*), fatty acid synthase (*Fas*), stearoyl-CoA desaturase-1 (*Scd1*), long-chain elongase (*Elovl6*), fatty acid translocase (*Fat*). Fasting significantly reduced the levels of acetylated H3K9 on the promoter regions of *Gk*, *Lpk*, *Fat*, *Acc1*, *Fas*, *Elovl6*, and *Scd1* in the livers of wild-type mice, but was significantly abrogated in SIRT6-deficient livers. Another report by Yang *et al.* (137) showed that Rosiglitazone treatment (a thiazolidinedione-class, insulin-sensitizing drug commonly used for the treatment of T2DM) ameliorated hepatic lipid accumulation, increased SIRT6, PGC-1α and FOXO1 expression and altered the phosphorylation status of LKB1 and AMPK leading to activation of AMPK in rat livers. However,

knockdown of SIRT6 abrogated these effects, suggesting that they are SIRT6-dependent. Remarkably, these phenotypes in SIRT6-deficient livers are strikingly similar to the phenotypes observed in two distinct liver-specific SIRT1-deficient mouse models (77, 83). Interestingly, Kim *et al.* (51) discovered that SIRT1 forms a transcriptional complex on the *Sirt6* promoter with FOXO3a and nuclear respiratory factor-1. This complex positively regulates SIRT6 expression in response to caloric deficit. This mechanism may partly explain the increase in SIRT6 levels during fasting and CR and some of the similar effects of SIRT1 and SIRT6 deficiency. Consistent with this model, they observed a stark increase in SIRT1 levels within 12 hours of fasting followed by a significant increase of SIRT6 levels within 18 hours of fasting. These data suggest that in response to caloric deficit, SIRT6 is transcriptionally induced by SIRT1 and negatively regulates glycolysis and triglyceride synthesis in the liver by deacetylating H3K9 on promoters of specific genes involved in these processes.

This involvement of SIRT1 is perhaps not unexpected, as SIRT1 has previously been shown to be a regulator of HGP. SIRT1 was shown to deacetylate and activate PGC-1α, leading to induction of gluconeogenic transcriptional program (76, 82, 138). PGC-1α contains at least 13 acetylation sites, the acetylation of which are associated with repression of PGC-1α activity (76). In opposition to SIRT1, general control nonrepressed protein 5 (GCN5) acetylates and deactivates PGC-1α's transcriptional activity. In general, during energy abundance, acetylation of PGC-1α by GCN5 is favored, thus diminishing HGP. During periods of energy deficiency, deacetylation of PGC-1α by SIRT1 is favored leading to increased HGP (76, 139). Dominy *et al*. (140) recently demonstrated that depletion of SIRT6 reduces the acetylation status of PGC-1α and promotes upregulation of gluconeogenic gene transcripts and hepatic glucose production. Additionally, SIRT6's effect on PGC-1α acetylation status is GCN5-dependent. They further show that SIRT6 selectively deacetylates K549 on GCN5, leading to altered phosphorylation status and activation of GCN5. These data suggest that SIRT6 induces PGC-1α acetylation and suppresses hepatic gluconeogenesis in direct opposition to SIRT1 through deacetylation and activation of GCN5. The physiological significance for the opposing roles of SIRT1 and SIRT6 on

PGC-1α-mediated gluconeogenesis needs further investigation. However, it is interesting to note that activation of PKA signaling by either forskolin or glucagon in primary hepatocytes significantly reduced the expression of SIRT6 in opposition to the upregulation of SIRT6 by fasting, even though glucagon levels rise during fasting. This is suggestive of more complex regulation of SIRT1 and SIRT6 expression during fasting vs. prolonged caloric deficiency. Interestingly, Dominy *et al.* also reported that leptin receptor-deficient ($LepR^{db/db}$) diabetic mice, which exhibit hyperglucagonemia and chronic hepatic PKA activation (141), also exhibit reduced SIRT6 levels, while ectopic expression of SIRT6 in these animals ameliorated the hyperglucagonemia and normalized glycemia. This finding suggest that in opposition to SIRT1, overexpression of SIRT6 within the liver may be therapeutically efficacious for ameliorating the unrestrained HGP associated with insulin-resistant T2DM.

The investigation of SIRT6 function has predominantly come from tissue-specific SIRT6 deletion and whole-body knockout mouse models. However, in opposition with these strategies, Kanfi *et al.* (4) reported the findings of a ubiquitous transgenic SIRT6 overexpression (Sirt6-tg) mouse model. Wild-type and Sirt6-tg mice were fed either chow diet or a high-fat diet. They did not observe any significant differences in food intake, body weight, leptin or oxygen consumption between geneoptypes. However, they did observe significantly reduced LDL cholesterol in both chow diet- and high-fat diet-fed SIRT6 overexpression mice. They also observed reduced visceral fat accumulation and reduced triglyceridemia in Sirt6-tg overexpression mice on high-fat diet only. They did not observe altered insulin tolerance in either dietary regimen. However, they found that high-fat diet-fed mice had enhanced glucose tolerance and enhanced glucose-stimulated insulin secretion. Additionally, they observed significant downregulation of a subset of PPARγ-responsive genes involved in lipid storage and also genes involved in triglyceride synthesis including angiopoietin-like protein 4 (*Angptl4*), adipocyte fatty acid-binding protein (*Fabp4*), and diacylglycerol acyltransferase 1(*Dgat1*). This result is consistent with the previously discussed function of SIRT6 to inhibit triglyceride synthesis in the liver (51). These data suggest that SIRT6 protects against high-fat diet-induced dyslipidemia, visceral fat accumulation and impairment of

glucose homeostasis, and suggest that SIRT6 overexpression may be efficacious for the treatment of diet-induced obesity and T2DM.

However, as will be discussed in chapter two, several pieces of experimental evidence suggest incongruous interpretations regarding the functions of SIRT6. Additionally, substantial caveats inherent to these mouse models lead to disagreement regarding whether activation or inhibition of SIRT6 with a systemic-acting drug should be sought after and developed for the treatment of metabolic syndrome and T2DM. This rationale will be used to introduce the experimental "Sirt6BAC" SIRT6 overexpression mouse model developed and utilized in this work. I hypothesize that SIRT6 gain-of-function via overexpression will produce desired effects beneficial for the treatment of T2DM, which mirror those observed during caloric restriction including improved glucose homeostasis and enhanced insulin sensitivity.

CHAPTER TWO:

Generation of the "Sirt6BAC" Mouse Model and Validation of SIRT6 Overexpression/Gain-of-Function in Sirt6BAC Mice.

2.1 Introduction

The physiological and homeostatic functions of mammalian SIRT6 have been dissected with a variety of whole-body and tissue-specific manipulations in mice. While these investigations have proved greatly beneficial to our understanding of the role of SIRT6, important questions remain. Perplexingly, interpretations about the homeostatic roles of SIRT6 has shown to be more convoluted than expected, as certain *in vivo* metabolic phenotypes observed in these opposing loss-of-function/gain-of-function, whole-body and tissue-specific manipulations have suggested apparently incongruous interpretations of its homeostatic and metabolic functions, leading to uncertainty about whether SIRT6 activation or inhibition should be the goal in treating obesity and insulin resistance.

Specifically, whole-body *Sirt6* knockout mice (*Sirt6*$^{-/-}$) exhibit reduced body weight, reduced adiposity, hypoglycemia and die within the first few months of age (3, 123). SIRT6 deficiency also causes attenuated transcriptional silencing of genes involved in glycolysis and glucose transport (125, 142). According to these observations, downregulation of SIRT6 reduces adiposity, increases cellular glucose uptake and utilization, and consequently reduces glycemia. Therefore, whole body SIRT6 upregulation should increase adiposity, decrease cellular glucose uptake and utilization and consequently increase glycemia. However, in contrast to this prediction, Kanfi *et al.* (4) demonstrated that SIRT6 overexpression in Sirt6-tg mice is able to reduce visceral fat accumulation and glucose intolerance brought on by a high-fat diet. One potential explanation for these conflicting whole-body effects could be due to disproportionate relative contributions to whole body adiposity and glucose homeostasis depending upon the relative expression levels and activity of SIRT6 in each cell type. This possibility is particularly relevant due to the fact that the aforementioned SIRT6 overexpression model (4) is driven by a ubiquitous *βActin* promoter, which does not possess any of the transcriptional regulatory elements found in the

endogenous *Sirt6* promoter, thus leading to aberrant relative SIRT6 expression in various cell-types. This rationale may suggest that the contributions to whole-body glycemia and adiposity are disproportionately overrepresented by this overexpression model in cell-types that normally weakly express SIRT6 and underrepresented by this overexpression model in cell-types that normally strongly express SIRT6.

Even so, this issue can be alleviated by studying the effects of SIRT6 manipulations in a cell-type-specific manner, which has been done in neurons (120), cardiomyocytes (123), and hepatocytes (51). Hepatic-specific *Sirt6*-knockout mice exhibit elevated expression of genes involved in lipogenesis and triglyceride storage, resulting in fatty liver (51). This observation also leads to in conflicting interpretations of SIRT6 function when comparing it against the dramatic reduction of body fat in the whole body *Sirt6*$^{-/-}$ mouse model. Furthermore, Dominy *et al.* (140) demonstrated that SIRT6 inactivates PGC-1α through deacetylation of GCN5 leading to suppressed gluconeogenesis, suggesting that SIRT6 should reduce glycemia by inhibiting hepatic glucose production. However, this does not appear to coincide with the very low glucose levels observed in the whole body *Sirt6*$^{-/-}$ mouse.

Additionally, Sundaresan *et al.* (123) showed that SIRT6 attenuates IGF1-AKT intracellular signaling in cardiomyocytes and protects against cardiac hypertrophy, suggesting that SIRT6 inhibits growth. Xiao *et al.* (133), also demonstrated that SIRT6-deficiency leads to activation of AKT via upregulation of upstream proteins including InsR, IRS1, and IRS2. Consistent with these data, Kanfi *et al.* (5) reported that transgenic SIRT6 overexpression in Sirt6-tg mice leads to decreased serum IGF1 levels and altered phosphorylation of major components of the IGF1-AKT signaling pathway associated with reduced IGF1-AKT signaling. However, these results do not appear to fit with the small size and reduced GH/IGF1 levels of systemic *Sirt6*$^{-/-}$ mice and neural-specific SIRT6-deficient mice.

These incongruous interpretations regarding the homeostatic functions of SIRT6 cast doubt as to whether SIRT6 agonist or antagonist drugs should be sought after for the treatment of obesity and/or T2DM. One possible explanations for these apparently contradictory results may include confounding effects of the multifaceted aberrancies and developmental defects displayed by systemic *Sirt6*$^{-/-}$ mice including colitis, lymphopenia, osteopenia, kyphosis, malocclusion, and chromosome and telomere

abnormalities (3). If this is indeed a substantial confounding factor limiting the assessment of systemic SIRT6 function, which it is likely to be considering the severity of these phenotypes, then studying the reverse system, a SIRT6 overexpression model, may prove useful.

During prolonged CR and within 18 hours of acute fasting, the levels of SIRT6 are significantly upregulated between two- and three-fold within the brain, WAT, kidney, and heart (51, 52). This observation begs the question, whether certain beneficial metabolic effects elicited by CR may be caused by the increase in SIRT6 levels. Kanfi *et al.* (4) first demonstrated that Sirt6-tg mice exhibit many of the same beneficial metabolic effects as CR, and SIRT6 overexpression is able to protect against high-fat diet induced elevated LDL-cholesterol, visceral fat accumulation, elevated triglycerides, glucose intolerance and impaired glucose-stimulated insulin secretion. However, this particular Sirt6-tg mouse model reported in Kanfi *et al*. (4), exhibits several inherent caveats that cast doubt as to whether these effects are reflective of the physiological actions of SIRT6 when upregulated during CR. The particular SIRT6 overexpression construct chosen for this study used a CMV early enhancer/chicken βActin promoter (commonly used to drive transgene expression in mammalian systems (143, 144)) to drive expression of *Sirt6* cDNA. This system has four potential caveats. First, the CMV early enhancer leads to a very high supraphysiological level of expression – much higher than the two- to three-fold increased expression of SIRT6 observed during CR. Second, the chicken βActin promoter does not possess the same regulatory elements of the endogenous *Sirt6* promoter and should drive the *Sirt6* cDNA expression ubiquitously in all cell types to equal levels. Even though endogenous SIRT6 is present in all tissues examined, its expression levels vary in different cell-types. Thus, the ubiquitous expression of SIRT6 from the Sirt6-tg construct is different than the variable endogenous SIRT6 expression in different cell-types. Third, the use of *Sirt6* cDNA does not allow for the expression of any potential alternative transcriptional splice variants that may exist for the endogenous *Sirt6* gene. Indeed, NCBI Gene ID 50721 currently lists two alternatively spliced *Mus musculus Sirt6* transcripts (NM_181586.3 and NM_001163430.1) differing in the 5’ UTR, exon 1, exon 2 and 3’ UTR. Finally, the use of *Sirt6* cDNA does not incorporate the intronic

DNA regions of the endogenous *Sirt6* gene, which may also affect differential transcriptional regulatory function. Therefore, the ubiquitous, supraphysiological, constitutive expression is quite different from the natural expression driven by the endogenous *Sirt6* promoter.

In light of these caveats inherent to the existing SIRT6 mouse models, I sought to generate a SIRT6 overexpression mouse model that would: *i*) eliminate, or reduce the significance of these caveats, *ii*) overexpress SIRT6 in a more physiological manner than has been achieved with previous mouse models, *iii*) mimic the two- to three-fold upregulation of SIRT6 observed during CR, and *iv*) provide proof of principle that systemic SIRT6-activating drugs could be useful in the treatment of metabolic syndrome and T2DM.

2.2 Materials & Methods

Generation of Sirt6BAC mice:

A bacterial artificial chromosome (BAC) containing 185.7kb (70.7kb upstream and 109.3kb downstream) of unmodified mouse genomic DNA sequences including the mouse *Sirt6* gene (Figure 1A) (BAC clone RP23-352G18, BACPAC (BACPAC RESOURCES, CHILDREN'S HOSPITAL Oakland, CA, USA) was purified as previously described (145) and used as template sequence for PCR reactions with the primer sets shown in Primer Table 1. The size of the amplicons generated from these PCR reactions were analyzed via standard gel electrophoresis, in order to confirm that this was the expected BAC DNA clone. The purified BAC DNA was then electroporated into EL250 bacteria (146) and rendered electrocompetent as previously described (145). A loxP sequence(s) contained in the pBACe3.6 backbone of RP23-352G18 BAC was then replaced via homologous recombination (146) by an ampicillin resistance gene cassette, generated via PCR amplification of a PGEM-T-Easy vector template with the oligonucleotide PCR primers shown in Primer Table 2. With the expertise of the UT Southwestern Transgenic Core Facility, the modified RP23-352G18 BAC DNA was then purified and microinjected into pronuclei of fertilized embryos of C57Bl/6 mice using standard methods commonly used for generation of transgenic mice (147). PCR genotyping of tail biopsies from these offspring using primer

sets specific to the pBACe3.6 backbone sequence of RP23-352G18 (Primer Table 3), three mice were identified having germ-line incorporation of RP23-352G18 BAC DNA. These three founder mice were bred to wild-type C57Bl/6 mice to establish three distinct mouse lines. In order to determine which of these three lines would be appropriate for this study, the expression level of SIRT6 protein in these lines was measured via Western blot in various tissues from F1 generation mice of each of the three lines. Mice carrying the RP23-352G18 BAC DNA and wild-type control mice were fasted at 5pm and sacrificed the next morning at 10am. Tissues were dissected and flash frozen in liquid nitrogen. Protein lysates from these tissues were assessed by Western blot analysis.

Generation of Sirt6BAC mice lacking endogenously encoded SIRT6 (Sirt6BAC; *Sirt6*$^{-/-}$ mice):

Sirt6BAC mice (pure C57Bl/6 genetic background) were bred to mice heterozygous for the *Sirt6*-knockout allele (*Sirt6*$^{+/-}$)(pure 129SvJ genetic background) (provided by Raul Mostoslavsky M.D. Ph.D., Massachusetts General Hospital Cancer Center, Harvard Medical School). F1 offspring (C57Bl/6; 129SvJ mixed genetic background) were inbred (*Sirt6*$^{+/-}$ x Sirt6BAC; *Sirt6*$^{+/-}$) to generate F2 offspring. These inbred F2 offspring were employed as breeding pairs (*Sirt6*$^{+/-}$ x Sirt6BAC; *Sirt6*$^{+/-}$) to generate experimental mice for this study including: wild-type mice, mice harboring the Sirt6BAC insertion (Sirt6BAC), or mice harboring Sirt6BAC and homozygous for the *Sirt6* knockout allele (Sirt6BAC; *Sirt6*$^{-/-}$). To determine whether a mouse contained Sirt6BAC, I employed a PCR genotyping reaction using primers specific for a region on the pBACe3.6 backbone (Primer Table 3). To determine whether a mouse contained zero, one or two *Sirt6*-knockout alleles, I utilized a multiplex TaqMan qPCR copy-number genotyping assay produced by Applied Biosystems® (Foster City, CA, USA). Transferrin Receptor (Tfrc; Cat # 4458366 VIC dye-labeled probe) was used as endogenous reference copy-number and the the β-galactosidase (lacZ; Mr00529369_cn FAM dye-labeled probe) from Applied Biosystems® was used to quantify the *Sirt6* knockout allele copy number. Applied Biosystems® Copy Caller™ software was used to calculate the number of alleles present. Of note, β-galactosidase sequences were used to swap endogenous wild-type *Sirt6* sequences in *Sirt6*$^{+/-}$ mice (3). Thus, mice bearing two of the endogenous wild-type *Sirt6* alleles were found to have zero copies of the β-galactosidase allele, whereas mice bearing

one of the endogenous wild-type *Sirt6* alleles were found to have one copy of the β-galactosidase allele, and mice lacking both endogenous wild-type *Sirt6* alleles were found to have two copies of the β-galactosidase allele.

Western Blot Analysis:

Tissues from overnight fasted mice were lysed with RIPA buffer (R0278 Sigma Aldrich®) with 1:100 dilution of protease inhibitor cocktail (P8340 Sigma Aldrich®). Equal amounts of protein lysates (20μg) were separated via SDS-PAGE and transferred to nitrocellulose membranes as by electroblotting. Subsequently, the membranes were blocked using LI-COR® Odyssey® blocking buffer (927-40000) for 2 hours at room temperature, then placed in primary antibody incubation (rabbit polyclonal anti-SIRT6 [Abcam® ab62739] 1:3000 dilution and mouse monoclonal anti-βActin [Sigma Aldrich® A5316] or chicken polyclonal anti-αTubulin [Abcam® ab89984] 1:5000 dilution) in LI-COR® Odyssey® blocking buffer w/ 0.1% Tween-20, overnight at 4^{o}C. After washing the membranes 3x10 minutes in PBS w/ 0.1% Tween-20, they were incubated at room temperature in darkness for 2 hours with fluorescently conjugated secondary antibodies (goat anti-rabbit LI-COR® IRDye® 800CW [926-32211] 1:5,000 and goat anti-mouse LI-COR® IRDye® 680 [926-32220] 1:10,000 or donkey anti-chicken LI-COR® IRDye® 680RD [926-68075] 1:10,000) in Odyssey® blocking buffer w/ 0.1% Tween-20, 0.01%SDS. The membranes were imaged with a LI-COR® Odyssey® infrared imager. SIRT6 specific bands (~37kD) were quantified relative to anti-βACTIN (~42kD) or anti-αTUBULIN (~53kD) using LI-COR® Odyssey® Image Studio software.

Quantitative Real-Time PCR (qPCR) Analysis of Gene Transcripts on RP23-352G18:

Tissues from overnight fasted (mixed genetic background C57Bl/6;129SvJ) mice were lysed in TRIzol® reagent in order to extract total RNA. cDNA was reverse transcribed from these purified RNA samples with Invitrogen SuperScript® III reverse transcriptase as previously described (148). Genes present on RP23-352G18 BAC were assayed via real-time qPCR gene expression analysis to determine the levels of mRNA transcript expression. qPCR gene expression analysis was performed using

inventoried TaqMan gene expression assays (Applied Biosystems®). These genes included: *AES*(Mm01148854_g1), *Ankrd24*(Mm01147213_m1), *BC025920*(Mm02763635_s1), *Gna11*(Mm01172792_m1), *Gna15*(Mm00494669_m1), *Tle2*(Mm00498094_m1), *Tle6*(Mm00475103_m1), and *Sirt6*(Mm01149042_m1). Expression levels were measured with an Applied Biosystems® 7900HT Sequence Detection System with SDS2.1 software. Baseline values of amplification plots were set automatically and threshold values were kept constant. The mRNA levels were expressed as arbitrary units and were obtained by dividing the averaged sample values (in triplicate) for each gene by that of the control housekeeper 18S rRNA (Mm03928990_g1).

Animal Care:

Mice were housed with *ad libitum* access to food and water in light (12 hours on / 12 hours off) and temperature (21.5-22.5^{O}C) controlled environment. Male mice were used for all experiments and were housed 2-5 per cage. The maintenance chow diet was a 12 kcal% from fat, 22 kcal% from protein, and 66 kcal% from carbohydrate diet (Harlan Teklad® Global Diet #2916). Care of mice was within the Institutional Animal Care and Use Committee (IACUC) guidelines, and all the procedures were approved by the University of Texas Southwestern Medical Center IACUC.

Statistical Analyses:

The data are reported as mean ± SEM. All statistical analyses were performed using Prism (version 6.0) software. Unpaired two-tailed t-tests were employed when 2 groups were compared and one-way ANOVA with Tukey correction for multiple comparisons were employed when 3 or more groups were compared.

2.3 Results

I developed genetically engineered mice designed to overexpress SIRT6 by obtaining a commercially available bacterial artificial chromosome (BAC) containing unmodified, isogenic, genomic DNA from *Mus musculus* chromosome 10, which includes 70.7kb upstream and 109.3kb downstream of

the mouse *Sirt6* gene (Figure 1A). The BAC was purified and confirmed to be the correct clone (RP23-352G18) via conventional PCR genotyping of distal regions of the BAC. A single, functional loxP sequence contained in the pBACe3.6 backbone sequence was removed, to prevent any unwanted Cre recombinase-mediated mutations, and replaced with an ampicillin-resistance cassette. I observed a lack of any major rearrangements to the BAC nucleotide sequence by comparison of the restriction digest patterns of unmodified and loxP-replaced BAC DNA.

The modified BAC DNA was then purified and microinjected into pronuclei of fertilized embryos of C57Bl/6 mice to facilitate incorporation into the endogenous mouse genome, engendering these mice with additional copies of the mouse *Sirt6* gene. These offspring were genotyped using oligonucleotide primer pairs specific to the pBACe3.6 backbone sequence of RP23-352G18 (Primer Table 3) to confirm the presence of RP23-352G18 BAC DNA. Three mice were identified as having germ-line incorporation of RP23-352G18 BAC DNA. These three founder mice were bred to wild-type C57Bl/6 mice to establish three distinct RP23-352G18 mouse lines. In order to determine which of these three lines exhibited SIRT6 overexpression appropriate for this study, various tissues from F1 generation RP23-352G18 BAC mice of each of the three lines were examined via Western blot for SIRT6 protein expression. One of the three RP23-352G18 BAC mouse lines was found to exhibit between two to four times greater SIRT6 expression than control wild-type littermates in various tissues (Figure 1B, 1C), suggesting that the DNA sequences contained in the RP23-352G18 BAC include the crucial transcriptional regulatory elements of the endogenous *Sirt6* gene. Of note, this magnitude of SIRT6 overexpression observed in these mice approximates the level of SIRT6 upregulation observed in calorically restricted rodents (52). This "Sirt6BAC" mouse line exhibiting two to four-fold overexpression of SIRT6 protein was chosen.

The RP23-352G18 BAC contains a large amount of genomic mouse sequence (185.7kb). In addition to the *Sirt6* gene, the RP23-352G18 BAC contains other known mouse gene sequences including: *AES, Ankrd24, BC025920, Gna11, Gna15, Tle2,* and *Tle6.* Since these genes could also retain the transcriptional elements necessary for their expression, and potentially lead to phenotypes due to potential overexpression, I devised to generate a control genotype that would disassociate the

overexpression of SIRT6 from any potential overexpression of these other genes present on the RP23-352G18 BAC sequence. This was accomplished by breeding the Sirt6BAC mouse line (C57Bl/6 pure genetic background) with the *Sirt6*-knockout (*Sirt6*$^{-/-}$) mouse line (129SvJ pure genetic background). These breedings produced (C57Bl/6;129SvJ mixed genetic background) three experimental genotypes for use in this study: wild-type, mice harboring the RP23G18 BAC germline incorporation (Sirt6BAC), or mice harboring the RP23G18 BAC germline incorporation and homozygous for the *Sirt6*-knockout allele (Sirt6BAC; *Sirt6*$^{-/-}$). To confirm the relative expression of SIRT6 in these mixed genetic background (C57Bl/6;129SvJ) offspring, I performed Western blot analysis on gastrocnemius tissue from mice of these three genotypes (Figure 1D). I again observed significant overexpression of SIRT6 in Sirt6BAC mice, and this overexpression was significantly abrogated in SIRT6; *Sirt6*$^{-/-}$ mice (Figure 1E).

To investigate whether the other genes present on the RP23-352G18 BAC were similarly overexpressed, qPCR profiling of transcripts whose genes/coding regions are contained in the RP23-352G18 BAC was conducted. Not surprisingly, all of these genes were significantly overexpressed in brain, gastrocnemius muscle and liver of both Sirt6BAC and Sirt6BAC; *Sirt6*$^{-/-}$ mice compared to wild-type controls (Figure 1F). Importantly, in agreement with the roughly two- to four-fold SIRT6 protein overexpression observed in the C57Bl/6 Sirt6BAC line (Figure 1B, 1C), *Sirt6* mRNA was also found in this mixed genetic background (C57Bl/6 & 129SvJ) to be overexpressed roughly three-fold in brain, gastrocnemius and liver of Sirt6BAC mice compared to wild-type controls (Figure 1F). Of note, in Sirt6BAC; *Sirt6*$^{-/-}$ mice, *Sirt6* overexpression was significantly diminished, while the other genes remained similar compared to Sirt6BAC mice (Figure 1F). These data suggest that Sirt6BAC; *Sirt6*$^{-/-}$ genotype is an important and useful control genotype because it will allow for distinguishing between phenotypes (if any) seen in Sirt6BAC mice due to overexpression of SIRT6 and/or other genes contained in the BAC. If a given phenotype displayed by Sirt6BAC mice were to be absent in Sirt6BAC; *Sirt6*$^{-/-}$ mice, then, it is very likely that SIRT6 overexpression is required for the given phenotype to be present, whereas a phenotype present in both genotypes could be attributed to one of the other genes present in the RP23-352G18 BAC DNA sequence.

In order to further demonstrate that this Sirt6BAC mouse model not only overexpresses SIRT6, but overexpresses a functionally competent SIRT6 protein and is thus a SIRT6 gain-of-function model, the ability of Sirt6BAC to rescue the profound developmental phenotypes of *Sirt6*$^{-/-}$ mice were assessed. *Sirt6*$^{-/-}$ mice die within several weeks of age, are shorter in length and weigh less than wild-type mice(3). Presence of the Sirt6BAC in Sirt6BAC; *Sirt6*$^{-/-}$ mice was observed to rescue the postnatal lethality (Figure 2A), reduced length (Figure 2B) and weight (Figure 2C) of *Sirt6*$^{-/-}$ mice. These data demonstrate that the SIRT6 protein expressed from the Sirt6BAC sequence likely retains all of the functional properties of endogenously expressed SIRT6, as it is functionally competent to rescue the functions of endogenously encoded SIRT6, and that Sirt6BAC mice are indeed a SIRT6-gain-of-function model. Collectively, these data suggest that Sirt6BAC mice physiologically overexpress functionally competent SIRT6 protein.

2.4 Discussion

A "Sirt6BAC" mouse model was developed for the experimental investigation of SIRT6 overexpression. Importantly, SIRT6 protein was found to be overexpressed between 2- and 4-fold in various tissues of Sirt6BAC mice. These levels of SIRT6 overexpression are consistent with the level of SIRT6 upregulation during CR. This result suggests that the extra copies of the *Sirt6* gene present in the Sirt6BAC are sufficient to drive SIRT6 overexpression in a physiological manner, mimicking that which is observed during CR.

Additionally, the SIRT6 protein produced from extra *Sirt6* gene copies present on the Sirt6BAC are functionally competent, as the postnatal lethality, reduced size and reduced weight of *Sirt6*$^{-/-}$ mice was rescued by the presence of Sirt6BAC. This result suggests that SIRT6 produced by isogenic *Sirt6* sequences present in Sirt6BAC mice likely retains all of the enzymatic and functional properties of SIRT6 produced from the endogenous *Sirt6* gene locus.

As shown in Figure 2A, a minor percentage of *Sirt6*$^{-/-}$ mice survived longer than 4 weeks of age, an observation slightly different from the nearly complete lethality observed by Mostoslavsky *et al.* (3).

The increased resistance to postnatal lethality could be due to differences in genetic background, as the *Sirt6*$^{-/-}$ mice in Mostoslavsky *et al.* were a pure 129SvJ inbred strain, while the mice in the present study were of a mixed (129SJv / C57Bl/6) genetic background. Notably, a genetic background effect on early postnatal lethality displayed by *Sirt6*$^{-/-}$ mice was also shown by another group (123).

One significant caveat about this SIRT6 overexpression model is that, other genes present on the RP23-352G18 BAC in Sirt6BAC mice are also overexpressed. These overexpressed genes could potentially lead to phenotypes that are not SIRT6-dependent. Therefore, in addition to wild-type and Sirt6BAC genotypes I generated a third control genotype, Sirt6BAC; *Sirt6*$^{-/-}$, for use in this study. This genotype was observed to retain the overexpression of these non-*Sirt6* genes present on the RP23-352G18 BAC in brain, gastrocnemius and liver tissue. However, the overexpression of *Sirt6* mRNA and protein were significantly abrogated in this control genotype. These data suggests that Sirt6BAC; *Sirt6*$^{-/-}$ genotype is an important control because it distinguishes between phenotypes (if any) seen in Sirt6BAC mice due to overexpression of SIRT6 and/or other genes contained in the BAC. In fact, if a given phenotype displayed by Sirt6BAC mice were to be absent in Sirt6BAC; *Sirt6*$^{-/-}$ mice, then, it is very likely that SIRT6 overexpression is required for the presence of the given phenotype, whereas a phenotype present in both genotypes could be attributed to one of the other genes present in the RP23-352G18 BAC DNA sequence.

These data suggest that this Sirt6BAC eutopic SIRT6 overexpression model offers significant advantages over a previously reported Sirt6-tg SIRT6 overexpression model employing a CMV early enhancer/chicken βActin promoter driving ubiquitous SIRT6 overexpression previously reported by Kanfi *et al.* in 2010 (4). First, the Sirt6-tg model employs a CMV early enhancer region that drives very high supraphysiological level of SIRT6 expression, which is much higher than is observed during CR. The Sirt6BAC model does not exhibit this caveat, as we observed a moderate, physiological level of overexpression, consistent with that observed during CR. Secondly, the Sirt6-tg model employs a chicken βActin promoter that drives SIRT6 expression ubiquitously without regard for the natural pattern of

SIRT6 expression in various tissues because it does not possess the endogenous transcriptional regulatory elements of the endogenous *Sirt6* gene. The Sirt6BAC model does not share this feature, as the very large amount of upstream and downstream DNA sequence peripheral to the Sirt6 gene contained in the RP23-352G18 Sirt6BAC is very likely to contain all of the transcriptional regulatory elements of the endogenous *Sirt6* promoter region. Consistent with this, I observed variable levels of overexpression two- to four-fold overexpression in various tissues of Sirt6BAC mice. Thirdly, the Sirt6-tg model employs mouse *Sirt6* cDNA, and therefore does not possess the potential to express any alternatively spliced transcripts that may exist for the *Sirt6* gene. In contrast, the Sirt6BAC model contains all intronic regions of the mouse *Sirt6* gene and an isogenic *Sirt6* promoter region; therefore it does have the potential to express any alternatively spliced transcripts of the *Sirt6* gene. Lastly, the use of *Sirt6* cDNA in the Sirt6-tg lacks endogenous intronic regions of the endogenous Sirt6 gene that may contain additional transcriptional regulatory elements. The Sirt6BAC model does not share this caveat, as it contains isogenic *Sirt6* gene sequences containing all intronic regions.

Collectively, these data suggest that Sirt6BAC mice eutopically overexpress functionally competent SIRT6 protein. This allows for the experimental investigation regarding whether whole body SIRT6 overexpression/gain-of-function *per se* can mimic various metabolic phenotypes observed during CR.

CHAPTER THREE:

SIRT6 Overexpression/Gain-of-Function Improves Glucose Homeostasis

3.1 Introduction

A great deal of investigation into SIRT6 function has focused on its role on glucose homeostasis. Several models of SIRT6 manipulation have revealed effects on glucose homeostasis. Mostoslavsky *et al.* (3) first reported that whole-body *Sirt6*$^{-/-}$ mice display profound hypoglycemia, suggesting that SIRT6 inactivation can reduce glycemia. Zhong *et al.* (125) also reported that SIRT6 downregulates the transcriptional activity of HIF-1α via deacetylation of H3K9. *Sirt6*$^{-/-}$ cells exhibit increased membrane localization of GLUT1, increased cell-autonomous glucose uptake, increased glycolysis, increased lactate production and decreased oxygen consumption, also suggesting that SIRT6 inactivation can lower glycemia by increasing cellular glucose uptake and usage in glycolysis. Xiao *et al*. (133) also demonstrated that SIRT6 deficiency results in increased GLUT1 and GLUT4 membrane association, which enhances glucose uptake, suggesting that SIRT6 increases blood glucose. However, Dominy *et al.* (140) demonstrated that depletion of SIRT6 reduces the acetylation status of PGC-1α, resulting in upregulation of gluconeogenic genes and hepatic glucose production. These data suggest that SIRT6 lowers blood glucose by suppressing PGC-1α-induced hepatic glucose production. Also, Kanfi *et al.* showed that SIRT6 overexpression in Sirt6-tg mice enhanced glucose tolerance and enhanced glucose-stimulated insulin secretion in high-fat diet-fed mice, which does not appear to fit with the interpretations of SIRT6's effect on glucose homeostasis from *Sirt6*$^{-/-}$ mice.

In addition to the effects of SIRT6 manipulation on glucose homeostasis, Mostoslavsky *et al.* (3) also reported that whole-body *Sirt6*$^{-/-}$ mice display reduced growth. Both whole-body *Sirt6*$^{-/-}$ and neural-specific *Sirt6*-knockout mice display reductions in IGF1 levels, presumably explaining the small size of each. However, these data are in disagreement with data from Sundaresan *et al.* (123), which showed that deletion of *Sirt6* specifically in adult mouse hearts led to cardiac hypertrophy. In these SIRT6-deficient hearts, significantly increased amounts of proteins belonging to the IGF-AKT signaling pathway were

observed including: IGF1R, InsR, ERK1, AKT, FOXO1 and glycogen synthase kinase 3 suggesting that SIRT6 attenuates IGF1 intracellular signaling, leading to reduced growth. Furthermore, Kanfi *et al.* (5) reported that transgenic SIRT6 overexpression leads to decreased serum IGF1 levels and altered phosphorylation of major components of the IGF-AKT signaling pathway, consistent with reduced IGF-AKT signaling, suggesting that SIRT6 inhibits growth. Again, these data suggests opposite effects of SIRT6 on growth regulation.

In addition to the effects of SIRT6 manipulation of glucose homeostasis and growth, Mostoslavsky *et al.* (3) also reported that whole-body *Sirt6*$^{-/-}$ mice display reduced adiposity. However once again, the interpretation that SIRT6 increases adiposity is not in agreement with the interpretation of SIRT6's function from data gleaned from other models of SIRT6 manipulation. Kim *et al.* (51) reported that deletion of *Sirt6* specifically in liver hepatocytes resulted in fatty liver with upregulation of genes involved in triglyceride synthesis including: *Acc1*, *Fas, Scd1*, *Elovl6* and *Fat*. Fasting significantly reduced the levels of acetylated H3K9 on the promoter regions of *Gk, Lpk, Fat, Acc1*, *Fas, Elovl6,* and *Scd1* in the livers of wild-type mice, but was significantly abrogated in SIRT6-deficient livers, suggesting that SIRT6 acts to suppress lipogenesis and fat storage. Schwer *et al.* (120) also found that neural-specific SIRT6-deficiency attenuated growth, but these mice ultimately became obese later in life. Additionally, Kanfi *et al.* reported that Sirt6-tg mice fed a high-fat diet were protected against visceral fat accumulation and hypertriglyceridemia, and displayed significant downregulation of a subset of PPARγ-responsive genes involved in lipid storage and triglyceride synthesis including: *Angptl4*, *Fabp4*, *Dgat1*. Once again, these data do not appear to fit with the interpretation of SIRT6's effect on lipogenesis from *Sirt6*$^{-/-}$ mice.

How can opposing models of SIRT6 manipulation have the same effects of lowering blood glucose, reducing growth/growth signaling and reducing fat accumulation/lipogenesis? Could these discrepancies be due to the aberrant, ubiquitous, and supraphysiological SIRT6 expression exhibited by Sirt6-tg mice reported by Kanfi *et al.*? Alternatively, could these discrepancies be due to opposing cell-autonomous vs. systemic mechanisms that only become dominant with SIRT6 upregulation or *vice versa*? Does complete lack of SIRT6 engender a completely different phenotype from only partial SIRT6

downregulation? Does SIRT6 have opposing effects in different tissues or cell-types? These are questions that need answers in order to determine the potential efficacy of targeting SIRT6 for the treatment of obesity and T2DM.

In order to answer some of these critical questions and investigate the effects of eutopic, physiological overexpression of SIRT6 on metabolic homeostasis, I employed the Sirt6BAC eutopic SIRT6 overexpression/gain-of-function model discussed in chapter two. I compared the metabolic profiles of these mutants with those of their littermate controls in the context of normal chow diet or high caloric diet (HCD) feeding conditions beginning at 8 weeks of age.

3.2 Materials & Methods

Body Weight and Body Composition Analysis:

Mice were weighed every other week beginning at 8 weeks of age. Body composition was determined monthly beginning at 8 weeks of age using the EchoMRI-100™ quantitative nuclear magnetic resonance system providing precise measurements of whole body fat and lean mass.

Analysis of Blood Glycemia and Serum Insulin:

Mice were singly housed in the morning (9am-12pm) in cages with fresh bedding and access to water, but without food during this time period to ensure that the experimental measurements were not affected by postprandial effects. Glycemia measurements were taken from tail blood samples with a OneTouch® Ultra® 2 glucometer with OneTouch® Ultra® Blue Test Strips. Immediately following, 50uL of blood was collected in tubes at room temperature for five minutes before placing into ice. The blood samples were then centrifuged at 2,000xg for 10 minutes at 4^{O}C. The blood serum supernatant was then pipetted into a new tube for storage at -80^{O}C. Insulin was measured by ELISA (Ultra Sensitive Mouse Insulin ELISA Kit Cat#90080, Crystal Chem, Inc.) from blood serum.

Intraperitoneal Glucose Tolerance Tests:

Intraperitoneal glucose tolerance tests (IPGTT) were performed in male, age-matched mouse cohorts with similar body weights. Mice were singly housed and fasted overnight (6pm-10am) in cages

with fresh bedding and access to water, but without food during this time period to ensure that the experimental measurements were under fasting conditions. An hour before the in vivo experiment, mice were weighed to determine the dosage of glucose to be administered (1.5g per kg bodyweight). Just prior to the injecting the glucose bolus, fasting glycemia was measured from tail blood samples with an AlphaTRAK blood glucometer. The glucose solution (0.15g glucose / mL 0.9% saline) was then injected into the intraperitoneal cavity of each mouse. Blood glucose measurements were taken from tail blood samples at t = 15, 30, 60, 90, and 120 minutes.

Intraperitoneal Pyruvate Tolerance Tests:

Intraperitoneal pyruvate tolerance tests (IPPTT) were performed in male, age-matched mouse cohorts with similar body weights. Mice were singly housed and fasted overnight (6pm-10am) in cages with fresh bedding without food, but with access to water during this time period to ensure that the experimental measurements were under fasting conditions. An hour before the in vivo experiment, mice were weighed to determine the dosage of pyruvate to be administered (2g per kg bodyweight). Just prior to the injecting the pyruvate bolus, fasting glycemia was measured from tail blood samples with an AlphaTrak blood glucometer. The pyruvate solution (0.2g sodium pyruvate / mL 0.9% saline) was then injected into the intraperitoneal cavity of each mouse. Blood glucose measurements were taken from tail blood samples at t = 15, 30, 60, 90, and 120 minutes.

Animal Care:

Mice were housed with *ad libitum* access to food and water in light (12 hours on / 12 hours off) and temperature (21.5-22.5^{O}C) controlled environment. Male mice were used for all experiments and were housed in groups of 2-5 per cage. The regular chow diet was a 12 kcal% from fat, 22 kcal% from protein, and 66 kcal% from carbohydrate diet (Harlan Teklad® Global Diet #2916). Mice in HCD cohorts were fed a 58.0 kcal% from fat, 16.4 kcal% from protein, and 25.5 kcal% from carbohydrate (12.6 kcal% from sucrose) diet (Open Source Diet Product #D12331 Research Diets Inc.) beginning at 8 weeks of age. Care of mice was within the Institutional Animal Care and Use Committee (IACUC)

guidelines, and all the procedures were approved by the University of Texas Southwestern Medical Center IACUC.

Statistical Analyses:

The values are reported as mean ± SEM. All statistical analyses were performed using Prism (version 6.0) software. Repeated measures two-way ANOVA with Tukey correction for multiple comparisons statistical analysis were employed when 3 groups were compared in longitudinal experiments. One-way ANOVA with Tukey correction for multiple comparisons statistical analyses were employed when 3 groups were compared.

3.3 Results

Sirt6BAC mice exhibit normal energy balance:

I assessed biweekly, the body weight of Sirt6BAC mice and their littermate wild-type and Sirt6BAC; *Sirt6*$^{-/-}$ controls fed either on a standard chow or HCD. In both chow and HCD feeding regimens, body weight was not significantly different between genotypes (Figure 3A, 3D). Additionally, body fat mass and lean mass were measured monthly by quantitative nuclear magnetic resonance. Both body fat mass (Figure 3B, 3E) and body lean mass (Figure 3C, 3F) were not found to be significantly different in normal chow diet and HCD feeding regimens. Together, these data demonstrate that eutopic, physiological overexpression of SIRT6 neither affects energy homeostasis nor protects from, or predisposes to, developing HCD-induced obesity.

Sirt6BAC mice exhibit reduced basal glycemia without alterations in basal insulinemia:

I also assessed basal (non-postprandial) glycemia at 8, 16 and 20 weeks of age. Significant alterations in basal glycemia were not found at 8 weeks of age in mice fed normal chow diet prior to 8 weeks of age (Figure 4A). However, at 16 weeks of age, Sirt6BAC mice in the chow diet context were found to exhibit modest, but significantly reduced basal glycemia compared with their wild-type littermates (Figure 4B). Additionally, at 16 weeks of age, Sirt6BAC mice fed on the HCD context were

found to exhibit reduced basal glycemia compared with their wild-type and Sirt6BAC; *Sirt6*$^{-/-}$ littermate controls (Figure 4B). Yet, at 20 weeks of age, I did not observe significant reductions in basal glycemia in either diet context. I also assessed basal (non-postprandial) insulinemia at 16 weeks of age in both diet contexts. Basal insulinemia was not found to be significantly altered in mice fed in either the normal chow diet or HCD context (Figure 4C).

Sirt6BAC mice exhibit enhanced glucose tolerance in the HCD context:

I assessed the ability of these mice to tolerate hyperglycemia in the chow diet context at 11-13 weeks of age and in the HCD context at 18-20 weeks of age via IPGTTs. Sirt6BAC mice in the chow diet context exhibited lower blood glucose levels than wild-type littermate controls at 30' and 60' times points, and lower blood glucose levels than Sirt6BAC; *Sirt6*$^{-/-}$ littermate controls at 15', 30' and 60' time points (Figure 5A). Although, Sirt6BAC mice in the chow diet context did not exhibit significantly enhanced glucose tolerance over the entire time course, as assessed by area under the curve (Figure 5B), however a trend toward enhanced glucose tolerance was noted in these mice. These effects became more apparent in the HCD context at 18-20 weeks of age. Sirt6BAC mice in the HCD context exhibited lower blood glucose levels than wild-type littermate controls at 15', 30' and 60' times points (Figure 5C). Sirt6BAC mice in the HCD context exhibited significantly enhanced glucose tolerance over the entire time course, as assessed by area under the curve (Figure 5D).

Sirt6BAC mice exhibit enhanced pyruvate tolerance in the HCD context:

I assessed the ability of these mice to tolerate a bolus of the gluconeogenic metabolite, pyruvate, in the chow diet context at 25-26 weeks of age and in the HCD context at 26-28 weeks of age via IPPTT. In the chow diet context, I did not observe significantly altered blood glucose levels at any time point (Figure 6A), nor did I observe significantly enhanced pyruvate tolerance over the entire time course as assessed via area under the curve (Figure 6B). However, I observed a profoundly significant phenotype in the HCD context at 26-28 weeks of age. Sirt6BAC mice in the HCD context displayed highly significant attenuated elevation of blood glucose levels relative to wild-type littermate controls at 30', 60', 90', and 120' time points, and relative to Sirt6BAC; *Sirt6*$^{-/-}$ littermate controls at the 30' time point (Figure 6C).

Sirt6BAC; *Sirt6*$^{-/-}$ mice also exhibited significantly attenuated elevation of blood glucose relative to wild-type littermate controls at 60', 90', and 120' time points. Sirt6BAC and Sirt6BAC; *Sirt6*$^{-/-}$ mice in the HCD context exhibited significantly enhanced pyruvate tolerance over the entire time course, as assessed by area under the curve (Figure 6D).

3.4 Discussion

Various models of SIRT6 manipulation discussed earlier, exhibit profound effects on growth, fat accumulation and glucose homeostasis. However, these models provide incongruous interpretations regarding the specific physiological effects of SIRT6 due to inherent caveats of these specific models. In order to bring the physiological functions of SIRT6 into greater focus, and to elucidate the effects of eutopic SIRT6 overexpression/gain-of-function on metabolic homeostasis, I employed the Sirt6BAC eutopic SIRT6 overexpression/gain-of-function model discussed in chapter two. I compared the metabolic profiles of these mutants with those of their wild-type and Sirt6BAC; *Sirt6*$^{-/-}$ littermate controls in the context of normal chow diet or HCD feeding conditions beginning at 8 weeks of age.

To determine the effects of eutopic, physiological overexpression/gain-of-function of SIRT6 on energy balance, I measured body weight, fat mass, and lean mass. I did not observe significant alterations in any of these measures in either diet context, suggesting that SIRT6 overexpression neither affects body weight or composition, nor protects from, or predisposes to, developing HCD-induced obesity. However, I cannot rule out potential effects beyond 20 weeks of age in the chow diet context or beyond 24 weeks of age in HCD context. These data are consistent with the report by Kanfi *et al.* (4) which did not find alterations in body weight homeostasis in Sirt6-tg model of SIRT6 overexpression. However, alterations in lipogenic gene expression and reduction of abdominal fat were observed in ectopic SIRT6-overexpressing mice, which is consistent with the effect of hepatic fat accumulation in a liver-specific *Sirt6* knockout model (51). These data are in disagreement with the data presented herein, showing a lack of an effect of SIRT6 overexpression on whole-body adiposity in either dietary regimen. However, if such an effect on adiposity is present in only a particular fat depot, it is possible that measurement of whole-

body adiposity is not sufficiently focused enough to observe a significant effect in male mice. Additionally, sexually dimorphic phenotypes are sometimes apparent in regard to adiposity. This cannot be ruled out in this case, as these studies were only conduced in males.

To determine the effects of eutopic, physiological overexpression/gain-of-function of SIRT6 on basal glycemia, I measured blood glucose levels at 8, 16, and 20 weeks of age in Sirt6BAC mice and their littermate wild-type and Sirt6BAC; *Sirt6*$^{-/-}$ controls in the standard chow diet and HCD contexts. I did not observe significant alterations in basal glycemia at 8 or 20 weeks of age in either diet context, though Sirt6BAC mice trended slightly lower than their age-matched littermate controls. However, at 16 weeks of age, significant, but modest reductions in basal glycemia were observed in Sirt6BAC mice relative to their littermate controls in both diet contexts, suggesting that SIRT6 overexpression modestly lowers basal glycemia. Insulin has the effect of lowering blood glucose. Therefore, to determine if these reductions in basal glycemia were associated with altered insulinemia, serum insulin levels were measured at 16 weeks of age. Significant alterations in serum insulin were not observed, suggesting that the reduction in basal glycemia in Sirt6BAC mice at 16 weeks of age is not due to altered insulinemia.

This modest alteration in basal glycemia may be due to differences in glucose clearance from blood. Investigations of *Sirt6*$^{-/-}$ *in vitro* and *in vivo* models have shown that SIRT6 suppresses cell-autonomous glucose uptake and usage (3, 125, 133). To gather further insights, IPGTTs were performed on Sirt6BAC mice and their wild-type and Sirt6BAC; *Sirt6*$^{-/-}$ littermate controls in the chow diet context at 11-13 weeks of age and in the HCD context at 18-20 weeks of age. Considering the cell-autonomous nature of the reported effects of SIRT6-deficincy on glucose uptake, I performed IPGTTs rather than the more physiological oral glucose tolerance test to exclude any incretin effects associated with glucose ingestion. I did not observe significant alteration in glucose tolerance in the chow diet context as assessed by area under the curve, although significant reductions in blood glucose were seen at various individual time points. These differences became far more apparent in the HCD context, where significantly enhanced glucose tolerance was seen in Sirt6BAC mice as assessed by area under the curve. Additionally, an intermediate phenotype was observed at several time points in Sirt6BAC; *Sirt6*$^{-/-}$ controls. Consistent

with an intermediate level of SIRT6 protein and *Sirt6* mRNA expression in the Sirt6BAC; *Sirt6*$^{-/-}$ genotype (Figure 1E, 1F), these data strongly suggest that SIRT6 overexpression, and not overexpression of other genes overexpressed from the Sirt6BAC DNA sequences engenders mice with enhanced glucose tolerance. These data are consistent with enhanced glucose tolerance in high-fat diet fed Sirt6-tg overexpressing mice reported by Kanfi *et al.* (4). However, these data are in disagreement with the interpretations from *in vitro* and *in vivo Sirt6*$^{-/-}$ models, which indicate that SIRT6 deficiency increases cell-autonomous glucose uptake.

SIRT6 has also been shown to be involved in the regulation of HGP via interactions with GCN5, an acetyltransferase that acetylates PGC-1α and suppresses its transcriptional activity on genes involved in gluconeogenesis. SIRT6 was shown to deacetylate and activate GCN5, causing acetylation and inactivation of PGC-1α, in opposition to the effects of SIRT1 (140). To gather further insights, I conducted IPPTTs with Sirt6BAC mice and their littermate wild-type and Sirt6BAC; *Sirt6*$^{-/-}$ controls in the chow diet context at 25-26 weeks of age and in the HCD context at 26-28 weeks of age. The ability of the IPPTT to reflect changes in hepatic glucose production has been demonstrated by several groups (82, 149, 150). Pyruvate is a central metabolite that intersects several metabolic pathways including being the principal substrate for gluconeogenesis. The glycemic response to a pyruvate bolus in the fasted state can be a good indicator of potential differences in the hepatic gluconeogenic pathway.

Mice in the chow diet context did not exhibit significantly enhanced pyruvate tolerance, although a trend toward enhance pyruvate tolerance was noted for Sirt6BAC and Sirt6BAC; *Sirt6*$^{-/-}$ mice (Figure 6B). Remarkably, 26-28 week-old Sirt6BAC and Sirt6BAC; *Sirt6*$^{-/-}$ mice in the HCD context displayed highly significant attenuated elevation of blood glucose levels relative to wild-type littermate controls at several time points (Figure 6C) and significantly enhanced pyruvate tolerance as assessed by area under the curve (Figure 6D). Additionally, Sirt6BAC; *Sirt6*$^{-/-}$ mice exhibited an intermediate area under the curve. Although the area under the curve of Sirt6BAC; *Sirt6*$^{-/-}$ mice was not significantly different from that of Sirt6BAC mice, a statistically significant attenuated elevation of blood glucose was observed in

Sirt6BAC mice relative to Sirt6BAC; *Sirt6*$^{-/-}$ controls at the 30’ time point. Consistent with an intermediate level of SIRT6 protein and *Sirt6* mRNA expression in the Sirt6BAC; *Sirt6*$^{-/-}$ genotype (Figure 1E, 1F), these data suggest that overexpression of SIRT6, and not overexpression of other genes overexpressed from the Sirt6BAC DNA sequences engenders mice with enhanced pyruvate tolerance. These data are consistent with the data from Dominy *et al.* (140) suggesting that SIRT6 suppresses hepatic gluconeogenesis. Collectively, these data suggest that SIRT6 overexpression *per se* provides protection against HCD-induced impairment of glucose homeostasis, but does not protect against, nor predisposes to HCD-induced obesity.

CHAPTER FOUR:

Sirt6BAC Mice Exhibit Enhanced Insulin Sensitivity

4.1 Introduction

Much of the investigations into SIRT6 function have focused on its role in glucose homeostasis. However, considering the principal role that insulin plays in controlling blood glucose levels, fairly little is known about SIRT6's insulin-responsive effects.

Several pieces of evidence suggest that SIRT6 affects insulin sensitivity. Insulin and IGF1 are endocrine hormones with high degree of sequence homology, and have complementary effects. IGF1 is secreted primarily by the liver in response to GH, and serves as a proliferative and growth signal, whereas insulin serves to direct whole-body glucose homeostasis and anabolic metabolism. Both hormones also share common intracellular signaling components such as IRS proteins, PI3K and AKT. Work by Xiao *et al.* (133) and Sundaresan *et al.* (123) demonstrated that SIRT6 deficiency leads to upregulation of several genes involved in the IGF1-AKT intracellular signaling pathway including: IGF1R, InsR, IRS1, IRS2, AKT, ERK1, and FOXO1, suggesting that SIRT6 decreases insulin sensitivity. Consistent with this interpretation, Kanfi *et al.* (5) reported that ubiquitous overexpression of SIRT6 in males leads to decreased IGF1 levels and altered phosphorylation of major components of the IGF1-AKT signaling pathway consistent with inhibited signaling. However, these mice did not exhibit altered insulin tolerance (4). Alternatively, Yang *et al.* (137) showed that knockdown of SIRT6 in hepatocytes abrogated the rosiglitazone (an insulin-sensitizing drug)-induced increases in PGC-1α and FOXO1 expression, and activation of AMPK, suggesting that they are SIRT6-dependent. Additionally, leptin receptor-deficient ($LepR^{db/db}$) diabetic mice exhibit reduced SIRT6 levels, while ectopic expression of SIRT6 ameliorates the hyperglucagonemia and normalizes glycemia (140), suggesting that SIRT6 is associated with insulin sensitivity. These data raise questions regarding whether activation or inhibition of SIRT6 would be efficacious for the treatment of insulin resistance in T2DM.

In chapter three, I demonstrated that SIRT6 overexpression appears to have glucose-lowering effects in IPGTTs, IPPTTs and on resting basal glycemia without alterations in basal insulinemia.

However, IPGTTs and IPPTTs may only help to guide further experiments into glucose homeostatic mechanisms, as they do not provide direct information regarding the ability of insulin to lower blood glucose.

Declining insulin sensitivity, progressing to insulin resistance is one of the hallmarks of T2DM. Insulin sensitivity is characterized by the insulin concentration in the blood required for a half-maximal response by peripheral tissues. In healthy, nondiabetic individuals, insulin has the effects of suppressing glucose production from the liver and kidneys, and promoting cellular glucose uptake (glucose disposal) and glucose metabolism particularly in glycolytic muscle and adipose tissue.

There are several experimental ways to test insulin sensitivity. The gold standard test for insulin sensitivity is the hyperinsulinemic-euglycemic clamp (HIEC) originally developed by DeFronzo *et al.* (151). The basic experimental setup involves defining the exogenous glucose (dextrose) infusion rate (GIR) that is able to "clamp" blood glucose in a physiologic range (euglycemic) in the context of supplying exogenous insulin to elicit hyperinsulinemia under steady state conditions (152). Although the HIEC is time consuming, labor intensive, expensive and requires an experienced operator, it offers significant advantages over other experimental methods such as insulin tolerance test and insulin suppression test. A HIEC directly measures whole body glucose disposal at a predetermined level of hyperinsulinemia under steady state conditions, whereas ITT involves additional assumptions due to not being at steady state conditions, leading to potential periods of hypoglycemia and ensuing counterregulatory homeostatic mechanisms such as gluconeogenesis, which insulin should suppress, not induce. The HIEC do not suffer these drawbacks. Another advantage of HIEC, is that radiolabeled glucose tracer ([3-^{3}H]glucose) can be used to quantify the rate of endogenous glucose production (EndoR_a) and the rate of whole body glucose disposal (R_d). Also, with the supplementation of a radiolabeled non-metabolizable glucose analog (2[^{14}C]deoxyglucose) in the steady state clamped condition, the absolute and relative glucose usage by specific peripheral tissues, as well as an assessment of whole body glycolytic rate can be calculated.

For these reasons, and to determine whether eutopic SIRT6 overexpression has a positive or negative effect (if at all) on insulin sensitivity, hyperinsulinemic-euglycemic clamps were performed in the Sirt6BAC mouse model of SIRT6 overexpression.

4.2 Materials & Methods

Hyperinsulinemic-Euglycemic Clamp:

Hyperinsulinemic-euglycemia clamp was performed in male, age-matched mice with similar body weights. 5 days prior to the *in vivo* experiment, mice were anesthetized using isoflurane and a catheter was surgically implanted in the right jugular vein and exteriorized above the neck as previously described (153). Hyperinsulinemic-euglycemic clamps were then performed in these 14-16 week old, conscious, unrestrained catheterized mice. Mice were fasted 5 hours prior to the start of the experiment (t = 0 min). At t = -120 min, an infusion of [3-^{3}H]glucose (0.05 μCi/min) was initiated. At t = -15 and -5 min, blood samples were collected from the tail vein to measure basal blood glucose and plasma insulin as well as to calculate the rate of endogenous glucose appearance (EndoR_a) and glucose disposal (R_d). At t = 0 min, a continuous insulin infusion (4 mU/kg bodyweight/min.) was used to induce hyperinsulinemia and the infusion of [3-^{3}H]glucose was increased to 0.1 μCi/min. Blood samples were then taken every 10 min to measure blood glucose and 50% dextrose was infused as needed to maintain target euglycemia (120 mg/dL). This target euglycemia was chosen because it was the average basal glycemia of the two groups. Additional blood samples were taken every 10 min from t = 100-120 min (steady state clamp) to determine plasma insulin and calculate glucose turnover. After the blood sample was taken at t = 120 min, a 12 μCi bolus of 2[^{14}C]deoxyglucose tracer was administered for the measurement of tissue-specific glucose uptake (R_g). Blood samples were obtained at t = 122, 130, 137, 145 minutes to assess blood glucose and 2[^{14}C]deoxyglucose specific activity. Mice were then anesthetized using pentobarbital and brain, BAT, liver, epididymal WAT, gastrocnemius, and soleus muscle were flash-frozen in liquid nitrogen for storage at -80°C for further analysis. Plasma concentrations of [3-^{3}H]glucose were determined following deproteinization of plasma samples with zinc sulfate and barium hydroxide. Basal

glucose turnover and insulin-stimulated R_d was determined as the ratio of the [3-^{3}H]glucose infusion rate to the specific activity of plasma [3-^{3}H]glucose at the end of basal period and during clamp steady state, respectively. EndoR_a during the clamp was determined by subtracting steady state GIR from R_d. R_g was determined by measuring the accumulation of phosphorylated 2[^{14}C]deoxyglucose in dissected tissues and the disappearance of 2[^{14}C]deoxyglucose from blood.

Animal Care:

Mice were housed with *ad libitum* access to food and water in light (12 hours on / 12 hours off) and temperature (21.5-22.5^{O}C) controlled environment. Male mice were used for all experiments and were housed in groups of 2-5 per cage. The regular chow diet was a 12 kcal% from fat, 22 kcal% from protein, and 66 kcal% from carbohydrate diet (Harlan Teklad® Global Diet #2916). Care of mice was within the Institutional Animal Care and Use Committee (IACUC) guidelines, and all the procedures were approved by the University of Texas Southwestern Medical Center IACUC.

Statistical Analyses:

The values are reported as mean ± SEM. All statistical analyses were performed using Prism (version 6.0) software. Repeated measures one-way ANOVA with Tukey correction for multiple comparisons statistical analysis were employed when 2 groups were compared in longitudinal experiments. Unpaired two-tailed t-tests were employed when 2 groups were compared.

4.3 Results

One possible explanation for the altered glucose homeostasis observed in Sirt6BAC mice presented in chapter 3, is enhanced sensitivity to the glucose-lowering effects of insulin. To test if increased insulin sensitivity underlies these phenotypes, hyperinsulinemic-euglycemic clamps were performed in 14-16 week old male Sirt6BAC and wild-type control littermates in the chow diet context. In agreement with the data presented in chapter 3, suggestive of underlying enhanced insulin sensitivity, the glucose infusion rate (GIR) (Figure 7A) required to clamp euglycemia (Figure 7B) was significantly increased in Sirt6BAC mice compared to wild-type control littermates. Basal endogenous glucose

appearance rate ($EndoR_a$) (Figure 7C) and basal glucose disposal rate (R_d) (Figure 7D) were not significantly different in Sirt6BAC mice compared with wild-type controls. However, during steady state hyperinsulinemic-euglycemic clamp, the ability of insulin to suppress endogenous glucose appearance was enhanced in Sirt6BAC mice compared with wild-type controls (Figure 7C). Indeed, $EndoR_a$ was completely suppressed in Sirt6BAC mice under steady state hyperinsulinemic-euglycemic conditions, whereas hyperinsulinemia only partially suppressed endogenous glucose production in wild-type controls. Similarly, during steady state hyperinsulinemic-euglycemic clamp, the ability of insulin to affect glucose disposal R_d was greatly enhanced in Sirt6BAC mice compared to wild-type controls (Figure 7D). Furthermore, the relative contribution to glucose disposal was measured in several tissues with the use of a radiolabeled glucose analog 2[^{14}C]deoxyglucose. Tissue-specific insulin-stimulated glucose uptake was significantly enhanced in Sirt6BAC mice in both gastrocnemius and soleus muscle, but not in brain, BAT or epididymal WAT (Figure 7E). The whole-body absolute glycolytic rate (not shown) and the glycolytic rate as percent of R_d (Figure 7F) were not significantly different between groups. Collectively, these data suggest that Sirt6BAC mice exhibit enhanced insulin sensitivity.

4.4 Discussion

Unfortunately, due to the time and labor intensive and expensive nature of HIEC experiments, Sirt6BAC; *Sirt6*$^{-/-}$ were unable to be included. Likewise, a cohort in the HCD feeding context was also unable to be completed. However, the data gleaned from experiments presented in chapter 3, suggest that the effects on glucose homeostasis are due to SIRT6 overexpression and not due to overexpression of the other genes present in Sirt6BAC DNA. Therefore, since a difference in insulin sensitivity can, and should affect these phenotypes in the predicted manner, it is a fairly reasonable to make the assumption that the effects observed in the hyperinsulinemic-euglycemic clamp in Sirt6BAC mice are as well, a result of SIRT6 overexpression and not due to overexpression of the other genes present in Sirt6BAC DNA. Additionally, since improved insulin sensitivity was observed in Sirt6BAC mice in the chow diet context, it is very unlikely that additional derangements posed by HCD feeding eliminate the differences observed

between SIRT6BAC mice and wild-types. Generally speaking, it is very common in overexpression models, that a given phenotype will only become apparent after stressing the physiology with HCD. In fact, the data present in chapter 3 on glucose homeostasis, where the phenotypes became more apparent in the HCD context, bears this out. Therefore, if hyperinsulinemic euglycemic clamps were to be performed in a HCD context with mice of both control genotypes, I would expect to observe even more significant differences between all three groups.

In spite of these shortcomings, the data presented in this chapter paints quite an intriguing picture regarding the functions of SIRT6 to control glucose levels in response to insulin. The truly powerful advantage about the hyperinsulinemic-euglycemic clamp is that the effects of insulin can be observed without the confounding effects of counterregulatory responses to dynamic changes in glycemia. Measurements at steady state ensure that the amount of exogenous glucose infused into the mouse in addition to the amount of endogenous glucose secreted into the blood must equal the amount of glucose leaving the bloodstream. Sirt6BAC mice were observed to require an elevated rate of glucose (dextrose) infusion (Figure 7A) to maintain euglycemia at 120 mg/dL (Figure 7B). This suggests that Sirt6BAC mice exhibit enhanced insulin sensitivity.

To determine whether the enhanced glucose-lowering effect due to hyperinsulinemia in Sirt6BAC mice comes primarily from enhanced cellular glucose glucose disposal (R_d) and/or from suppressing endogenous glucose appearance ($EndoR_a$) a radiolabeled glucose tracer isotope, [3-^{3}H]glucose was infused. Knowing the rate of glucose (dextrose) infused, the blood glucose at various time points, and the rate of [3-^{3}H]glucose infusion allowed for the calculation of the two remaining components determining blood glucose level: $EndoR_a$ and R_d. $EndoR_a$ was significantly blunted in Sirt6BAC mice compared with wild-type controls (Figure 7C), suggesting that the ability of insulin to suppress endogenous glucose appearance (likely coming from hepatic gluconeogenesis) was enhanced in Sirt6BAC mice. In fact, insulin was able to completely suppress endogenous glucose appearance in Sirt6BAC mice under steady state hyperinsulinemic-euglycemic conditions, whereas hyperinsulinemia only partially suppressed endogenous glucose appearance in wild-type controls. Also, R_d was observed to be significantly enhanced

in Sirt6BAC mice compared with wild-type controls (Figure 7D), suggesting that the ability of insulin to promote glucose transport into cells was also enhanced in Sirt6BAC mice. These data suggest that SIRT6 overexpression enhances the ability of insulin to suppress glucose production as well as to increase cellular glucose uptake. Though both of these arms were affected in Sirt6BAC mice, the relative contribution to the glucose lowering effect between Sirt6BAC mice and wild-type controls was more pronounced in R_d than EndoR_a, as R_d accounted for a ~13mg/kg/min., whereas EndoR_a only accounted for ~9mg/kg/min. difference between groups during steady state clamp.

In order to paint a more detailed picture regarding which specific tissues insulin promotes glucose uptake into, a low concentration of a radiolabeled glucose analog tracer, 2[^{14}C]deoxyglucose, was infused following the steady state clamp period at t = 120 minutes. 2[^{14}C]deoxyglucose is readily phosphorylated in the first step of glycolysis by glucokinase, but cannot be further metabolized and becomes trapped in most cells (excluding liver and kidney, which express glucose-6-phosphatase). This characteristic makes 2[^{14}C]deoxyglucose a good marker for tissue-specific glucose uptake (R_g) and rate of glycolysis (glucokinase activity). R_g was significantly increased in gastrocnemius and soleus muscle of Sirt6BAC mice, but not in brain, BAT or WAT (Figure 7E), suggesting that SIRT6 overexpression enhances the insulin-stimulated glucose uptake selectively in skeletal muscle. Although the relative difference in glucose uptake per gram of tissue in Sirt6BAC mice vs. wild-type mice was greater in soleus muscle (~30 μmol/100g tissue/min.) than gastrocnemius muscle (~5 μmol/100g tissue/min.), the relatively small total amount of soleus muscle compared to gastrocnemius muscle suggests that gastrocnemius muscle plays a more important role. However, why would soleus (an oxidative muscle fiber), transport more glucose than gastrocnemius (a glycolytic muscle fiber)? This is counterintuitive, as gastrocnemius, which is more heavily dependent upon glycolysis and much less energy efficient in terms of ATP production per glucose, would be expected to use more glucose than a more efficient oxidative muscle fiber such as soleus. Although, it is possible that, since soleus muscle uses very little glucose at basal, the relative difference in glucose usage upon insulin stimulation is greater in soleus due to enhanced insulin sensitivity in Sirt6BAC mice.

Significant differences in whole-body absolute glycolytic rate (not shown) were not observed in either the basal or hyperinsulinemic steady state. Since Sirt6BAC mice were observed to exhibit increased glucose disposal, thus have a greater supply of glucose substrate for glycolysis, the whole-body glycolytic rate was calculated as a percentage of R_d (Figure 7F). Still, a significant difference between groups was not observed in either the basal or hyperinsulinemic steady state, suggesting that whole body glycolysis is not altered in Sirt6BAC mice, or that a potential tissue-specific effect cannot be detected from the whole-body glycolytic calculation.

The data presented here are a mixed bag in regards to the effects of SIRT6 suggested by previously reported models of SIRT6 manipulation. Firstly, the enhanced insulin-stimulated suppression of glucose production ($EndoR_a$) is in agreement with data from Dominy *et al.* (140) suggesting that SIRT6 inhibits gluconeogenesis through deacetylation of GCN5. Additionally, these data are consistent with those indicating that the insulin-sensitizing effects of rosiglitazone are SIRT6-dependent (137).

However, previous reports of *in vitro*, whole-body, and tissue specific SIRT6 deficiency, lead to confusing interpretations when compared with the conclusions presented in this chapter. The data presented here indicate that SIRT6 enhances insulin-stimulated glucose disposal rate. This is appears to be in disagreement with *in vitro* and whole body *Sirt6*$^{-/-}$ models, which exhibit enhanced GLUT1 and GLUT4 membrane localization, and enhanced cell-autonomous glucose uptake (125, 133). However this may be explained by insulin insensitivity in these *Sirt6*$^{-/-}$ models, leading to disproportionately high glucose usage in the context of low insulin. Additionally, the lack of an observed effect on whole-body glycolytic rate does not support a previous report suggesting that SIRT6 downregulates glycolysis in mouse embryonic fibroblasts by transcriptionally silencing HIF-1α-regulated genes involved in glycolysis (125). However, in a separate report, SIRT6-deficient cardiomyocytes were not observed to exhibit any alterations in glucose uptake, glycemia, insulinemia, or changes in HIF-1α target genes *Pfk-1* and *Tpi-1* previously shown to be regulated by SIRT6. It is possible that, given the role of HIF-1α, these effects on

glycolytic gene regulation may only become apparent in response to hypoxia. Alternatively, potential cell-type dependent effects may be masked by whole-body measurement of glycolytic rate.

The physiological context in regards to energy status must be taken into consideration when interpreting these experiments. Specifically, the activity of Sirtuins and SIRT6 alike, are believed to be low in many tissues in the energy-replete, normoinsulinemic, normoglycemic state. Some Sirtuin-dependent effects may appear only when the physiology is stressed by fasting or CR. The HIEC experimental setup does not mimic the calorically deficient state, as blood glucose is available to tissues (though euglycemic) and insulinemia is high. Additionally, during periods when Sirtuin activity should be highest, such as fasting and CR, insulin levels are very low, whereas glucagon levels are very high. This point brings into question the physiological significance of insulin sensitivity during periods of caloric deficiency. Further experiments are needed to elucidate the mechanistic nature of these questions, which will be discussed in chapter 5.

CHAPTER FIVE:

Conclusions and Recommendations

5.1 Conclusions and Implications

Sirt6BAC mice were generated in order to test the hypothesis that eutopic SIRT6 overexpression, resulting in moderate, physiological SIRT6 gain-of-function could produce desired effects beneficial for the treatment of T2DM and/or obesity as well as provide proof of principal that SIRT6 agonist drugs may be worthy of translational research for the treatment of type-II diabetes in humans. I predicted that SIRT6 overexpression would mimic changes in physiology observed during caloric restriction including improved glucose homeostasis and enhanced insulin sensitivity. Sirt6BAC mice were generated via BAC-mediated genomic insertion of an isogenic 187kb DNA region from chromosome 10 of *mus musculus* encompassing *Sirt6.* One original founder line observed to exhibit moderate, CR-like 2 to 4-fold overexpression of SIRT6 in brain, pituitary, liver, WAT, and BAT was chosen for study.

Since the large DNA region of the Sirt6BAC also contained additional genes, a control genotype was needed to account for any potential phenotypes elicited by these other genes. Therefore, Sirt6BAC mice (a pure C57Bl/6 genetic background) were crossed with mice containing the *Sirt6*-knockout allele ($Sirt6^{+/-}$) (a pure 129SvJ genetic background). These offspring were bred for three generations to generate F3 mice for use in this study. This mixed genetic background (C57Bl/6; 129SvJ) containing the Sirt6BAC locus as well as the endogenous *Sirt6*-knockout allele, allowed for the study of three genotypes (wild-type, Sirt6BAC, and Sirt6BAC; $Sirt6^{-/-}$). Comparison of transcript expression from the genes present on the Sirt6BAC suggested that Sirt6BAC; $Sirt6^{-/-}$ mice are a valuable control genotype because they allow for the disassociation of SIRT6 overexpression from overexpression of the other non-*Sirt6* transcripts present on the Sirt6BAC. While Sirt6BAC mice were found to exhibit roughly 3-fold overexpression of *Sirt6*, Sirt6BAC; $Sirt6^{-/-}$ mice were found to exhibit only 2-fold overexpression of *Sirt6*. Thus, Sirt6BAC; $Sirt6^{-/-}$ displayed an intermediate level of *Sirt6* transcript expression, more than wild-type mice, but less than Sirt6BAC mice. A similar pattern of SIRT6 protein expression was observed in gastrocnemius muscle via Western blot. Therefore, Sirt6BAC; $Sirt6^{-/-}$ were shown to be a valuable control for this study,

because if a given phenotype displayed by Sirt6BAC mice were to be absent in Sirt6BAC; *Sirt6*$^{-/-}$ mice, then it is very likely that SIRT6 overexpression is required for the presence of the given phenotype, whereas a phenotype present in both genotypes could be attributed the other genes present in the RP23-352G18 Sirt6BAC DNA sequence. However, since an intermediate level of SIRT6 expression was found in Sirt6BAC; *Sirt6*$^{-/-}$ mice, intermediate phenotypes would be expected if it is SIRT6-dependent.

Additionally, this Sirt6BAC; *Sirt6*$^{-/-}$ genotype allowed for the determination of the functional competency of SIRT6 produced from the isogenic *Sirt6* gene present on the Sirt6BAC. Sirt6BAC; *Sirt6*$^{-/-}$ mice were observed to be rescued from the postnatal lethality, small size and reduced weight exhibited by *Sirt6*$^{-/-}$ mice (3). These data suggest that Sirt6BAC mice produce a functionally competent SIRT6 protein and are therefore a model of SIRT6 gain-of-function.

Next, the physiological and metabolic effects of SIRT6 gain-of-function were assessed in these three genotypes of male mice fed in the chow diet context or in the HCD context beginning at 8 weeks of age. The body weight, fat mass and lean mass were assessed and were not found to be significantly different between genotypes. This suggests that SIRT6 gain-of-function neither protects from, nor predisposes to HCD-induced obesity.

Knowing that previous models of SIRT6 manipulation had exhibited profound, but seemingly incongruent effects on glucose homeostasis, the Sirt6BAC model was employed to assess various indicators of glucose homeostasis. Firstly, basal glycemia was measured in these mice at 8, 16, and 20 weeks of age. These mice did not display significant alterations in basal glycemia at 8 and 20 weeks of age, although trends toward lower glycemia were noticed in Sirt6BAC mice, particularly in the HCD context. However, significant differences did show up at 16 weeks of age. In the chow diet context, a significant reduction in basal glycemia was observed between Sirt6BAC and wild-type mice. Additionally, in the HCD context, significant differences were observed between both Sirt6BAC mice and wild-type mice, as well as between Sirt6BAC mice and Sirt6BAC; *Sirt6*$^{-/-}$ mice, suggesting that SIRT6 overexpression *per se* accounted for these differences. Because differences in insulinemia could potentially explain the lower basal glycemia at 16 weeks of age, serum insulin levels were measured.

However, no differences in serum insulin were observed in either diet context. These data suggest that SIRT6 gain-of-function elicits effects that lower basal glycemia, but alterations in basal insulinemia are not one of them.

To further investigate the effects of SIRT6 gain-of-function on glucose homeostasis, IPGTTs were performed on these mice in both diet contexts. In the chow diet context, significantly lower blood glucose levels were observed in Sirt6BAC mice relative to both control genotypes at several time points after intraperitoneal glucose bolus, although these differences did not meet statistical significance over the entire time course as assessed by area under the curve. However, in the HCD context, significant differences were seen between Sirt6BAC mice and wild-types at several time points, as well as assessed by area under the curve. Although differences between Sirt6BAC mice and Sirt6BAC; *Sirt6*$^{-/-}$ mice did not reach statistical significance, a clear intermediate phenotype was noticed. An intermediate phenotype in Sirt6BAC; *Sirt6*$^{-/-}$ mice would be expected from the relative expression levels of SIRT6 in each genotype if the phenotype was caused by SIRT6 overexpression. Collectively, these data suggest that SIRT6 overexpression, and not overexpression of other genes overexpressed from the Sirt6BAC enhances glucose tolerance.

Next, to provide hints as to the gluconeogenic capacity of these mice, IPPTTs were performed in both diet contexts. In the chow diet context, significant differences were not observed, although trends toward enhanced pyruvate tolerance were observed in both Sirt6BAC mice and Sirt6BAC; *Sirt6*$^{-/-}$ mice. However, in the HCD context, profoundly significant differences between Sirt6BAC mice and wild-type littermates were observed at various time points in the IPPTT as well as by area under the curve. Also, an intermediate phenotype was observed in Sirt6BAC; *Sirt6*$^{-/-}$ mice, at both individual time points and as assessed by area under the curve. Together, these data suggest that SIRT6-gain-of-function is responsible for enhanced tolerance to the glycemia-elevating effects of pyruvate in the fasted state. This may be indicative of suppression of the gluconeogenic pathway in Sirt6BAC mice.

These phenotypes can all be caused by enhanced sensitivity to insulin. Insulin has glucose-lowering effects, by both stimulating cellular glucose uptake, as well as suppressing glucose production

from the liver and to a lesser extent, from the kidneys. To test whether Sirt6BAC mice exhibit enhanced insulin sensitivity, hyperinsulinemic-euglycemic clamps were conducted in the chow diet context in male wild-type and Sirt6BAC mice between 14-16 weeks of age. I observed significant increases in the glucose infusion rate required to maintain euglycemia. This is indicative of increased insulin sensitivity in Sirt6BAC mice. To further elucidate the specific reasons for the increased glucose requirement in hyperinsulinemic stead-state conditions, the endogenous glucose appearance rate and the rate of glucose disposal were calculated with the use of a radiolabeled [3-^{3}H]glucose tracer. Although significant differences were not seen between groups in the basal state, significant reduction in endogenous glucose appearance was observed in Sirt6BAC mice at clamped stead-state conditions suggesting that hepatic glucose production is suppressed in Sirt6BAC mice. This data supports the conclusion from IPPTT that hepatic gluconeogenesis is suppressed due to SIRT6 gain-of-function. Additionally, the rate of glucose disposal was increased in Sirt6BAC mice at clamped hyperinsulinemic steady state conditions, suggesting that insulin-stimulated cellular glucose uptake is enhanced in Sirt6BAC mice. This data supports data from IPGTTs suggesting that SIRT6 gain-of-function elicits enhanced cellular glucose uptake. Furthermore, with the use of a non-metabolizable glucose analog tracer 2[^{14}C]deoxyglucose, the tissue specific glucose uptake and whole body glycolytic rate were calculated. I observed significant insulin-stimulated increases in the tissue-specific glucose uptake in gastrocnemius and soleus muscle. This data suggests that muscle is the primary tissue of insulin-stimulated glucose uptake mediated by SIRT6 overexpression. Lastly, I did not observe significant reductions in whole-body glycolytic rate either in the basal or hyperinsulinemic-euglycemic clamped steady state.

Theses data offer a somewhat different picture of SIRT6 function than has been suggested by previous models of SIRT6 manipulation. SIRT6 gain-of-function in Sirt6BAC mice was not observed to elicit significant alterations in body weight or body composition. This does not support data from a whole-body *Sirt6*$^{-/-}$ mouse model which suggest that SIRT6 is required for normal growth, lipogenesis and fat accumulation (3). The growth phenotype was presumably accounted for by aberrancies caused by neuronal SIRT6-deficiency leading to low GH and IGF1 levels (120). Liver-specific and whole-body

Sirt6$^{-/-}$ elicited opposite effects on lipogenesis, however this may be due to the difference between cell-intrinsic effects and systemic (endocrine effects) of SIRT6-deficiency. Likely, SIRT6 suppresses lipogenic intracellular signaling, suggesting that the lack of fat accumulation in the whole-body *Sirt6*$^{-/-}$ model is secondary to the multitude of profound aberrancies associated with complete lack of SIRT6. Why, then are no significant effects on body composition seen in the Sirt6BAC overexpression model? Moderate manipulation of SIRT6 expression may be compensated for by alterations in GH, IGF1, insulin or other endocrine hormone sensitivity. Alternatively, moderate manipulation of its expression may not elicit a strong enough effect on these parameters to be detected by whole-body composition analysis, or that potential tissue-specific effects may be masked by the whole-body analysis.

SIRT6 gain-of-function in Sirt6BAC mice was demonstrated to elicit enhanced glucose tolerance, particularly in the HCD context. This finding is consistent with data employing Sirt6-tg male mice presented by Kanfi *et al*. (4, 5). However, the suggestion that SIRT6 gain-of-function engenders Sirt6BAC mice with enhanced insulin-stimulated glucose uptake into skeletal muscle may appear contradictory to *Sirt6*$^{-/-}$ *in vitro* models which display increased GLUT1 and GLUT4 membrane association and enhanced cell-autonomous glucose uptake (125), as well as *Sirt6*$^{-/-}$ *in vivo* models that display hypoglycemia in the context of low insulin and low IGF1 (3, 133, 154). It appears that the enhanced glucose uptake and usage in glycolysis is a cell-autonomous effect of SIRT6 deficiency. This suggests that SIRT6 serves to downregulate and inhibit intracellular IIS signaling pathway, which has been shown previously (5, 123, 125). If this is correct, why then, would SIRT6 overexpression in Sirt6BAC mice lead to enhanced glucose uptake? It is important to note that enhanced glucose uptake was not seen under normal insulin levels in the basal state, and that, only during the hyperinsulinemic-euglycemic clamp period was enhanced glucose disposal and enhanced muscle glucose uptake observed. If SIRT6 inhibits the IIS pathway at basal, normal insulinemic state, it may actually result in an enhanced capacity to respond to insulin's glucose lowering effect during hyperinsulinemia. SIRT6's effect to inhibit components of intracellular insulin signaling may actually be synonymous with enhanced insulin-sensitivity.

Sirt6BAC mice also exhibit attenuated elevation of blood glucose during IPPTT, and suppressed endogenous glucose production during HIEC, suggesting that SIRT6 gain-of-function enhances the ability of insulin to suppress hepatic gluconeogenesis. This is consistent with data from experiments demonstrating that SIRT6 silences a PGC-1α-mediated transcriptional program involved in gluconeogenesis by activating GCN5, which acetylates and inhibits PGC-1α (140). This would also lend support to the suggestion that SIRT6 increases insulin-sensitive effects, while inhibiting intracellular components at baseline.

The observation in this work that Sirt6BAC mice do not display alterations in overall whole-body glycolytic rate does not support the findings from *in vitro* data suggesting that SIRT6 silences a HIF-1α-mediated transcriptional program that enhances glycolysis (125). A potential explanation for this apparent disagreement could be that, given the role of HIF-1α, this phenotype may require a systemic stress such as hypoxia or caloric deficit to become apparent, neither of which should have been produced in the hyperinsulinemic-euglycemic clamp conditions where this measurement of whole-body glycolytic rate was made. Alternatively, potential tissue-specific effects may be masked by the whole-body measurement of glycolytic rate.

Lastly, the observations of elevated glucose infusion rate, enhanced glucose disposal rate and suppression of endogenous glucose production in hyperinsulinemic-euglycemic steady state conditions indicate that SIRT6 gain-of-function enhances insulin sensitivity. These data may appear to be in disagreement with data from published *Sirt6*$^{-/-}$ models, showing increased expression and altered phosphorylation status of proteins belonging to the IGF1-AKT intracellular signaling pathway consistent with activation of the pathway under basal conditions. Additionally, Kanfi *et al*. (5) also report that Sirt6-tg mice display decreased IGF1 levels and decreased phosphorylation status of p-IGF1R, p-AKT, p-FOXO1 in WAT of males, consistent with inhibition of IIS pathway. While these data clearly show inhibition of intracellular IIS signaling at basal state, they did not directly test the responsiveness to insulin. It is possible that enhanced IIS inhibition at basal state may also enhance the potential to become

activated in response to insulin. Supporting this line of thinking, SIRT6-deficient livers exhibited increased amounts of insulin responsive genes involved in glycolysis, as well as impaired sensitivity to insulin in insulin tolerance tests (51). More detailed experiments are needed to investigate the changes in the intracellular signaling giving rise to the enhanced insulin sensitivity observed in Sirt6BAC mice.

Overall, in contrast to various conclusions gleaned from experiments done in *Sirt6*$^{-/-}$ models, the data presented in this work demonstrate that, eutopic, physiological SIRT6 overexpression/gain-of-function has beneficial effects on glucose homeostasis: lowering basal glycemia, improving glucose tolerance, enhancing suppression of hepatic gluconeogenesis, which are all likely due to the observation of enhanced insulin sensitivity. These effects would all prove beneficial in the context of T2DM. Therefore, this research provides proof of principal that systemically acting SIRT6 agonist drugs could be an efficacious approach for the treatment of the various pathologies associated with T2DM.

5.2 Limitations of Present Work and Recommendations for Future Studies

One limitation of this study stems from the inherent makeup of the Sirt6BAC mouse model. Due to the need to preserve all the potential transcriptional regulatory sequences of the mouse *Sirt6* gene, a large BAC sequence was selected for use. A significant caveat to this approach is that several other genes are present in the large RP23-352G18 BAC DNA sequence used to generate Sirt6BAC mice, and are overexpressed in Sirt6BAC mice. Since the overexpression of these genes could lead to non-SIRT6-dependent phenotypes, I attempted to control for this caveat by introducing the *Sirt6*-knockout allele into the endogenous *Sirt6* gene locus. This approach allowed for the generation of a control genotype, Sirt6BAC; *Sirt6*$^{-/-}$, which was shown to maintain the overexpression of these non-*Sirt6* genes present in the RP23-352G18 BAC, but exhibited a significant reduction in both *Sirt6* transcript levels and SIRT6 protein from Sirt6BAC mice in several distinct tissues where SIRT6 is normally expressed. This approach proved to be useful for determining SIRT6-dependent phenotypes, as the intermediate level of *Sirt6* expression observed in Sirt6BAC; *Sirt6*$^{-/-}$ mice coincided with intermediate phenotypes on glucose homeostasis. This was to be expected if these phenotypes were SIRT6-dependent.

The second limitation of this study came as a result of introducing the *Sirt6*-knockout allele, which was contained in a distinct genetic background (129SvJ) from the original Sirt6BAC line contained in a pure C57Bl/6 genetic background. All the experimental mice in this study came from inbreeding of offspring from this original Sirt6BAC x *Sirt6*$^{+/-}$ mating. These study mice were from the F3 generation of mixed genetic background (C57Bl/6;129SvJ), meaning that there were just three rounds of meiotic genomic crossover and mixing from the original F0 founder mice. This relative lack of crossover events likely resulted in a high degree of heterogeneity in the genetic backgrounds of these study mice, which may have led to a high degree of variability in phenotypic analyses. Typically, 10 rounds of inbreeding are needed to ensure a relatively homogenous genetic background. However, due to cost and time constraints, it was not possible to generate study mice from further inbred generations to elicit more homogeneous genetic background. Therefore, it is recommended that future studies employ either the original Sirt6BAC line on a pure C57Bl/6 genetic background, or conduct experiments on these mixed genetic background mice in more heavily inbred generations to minimize the degree of heterogeneity in their genetic background.

Another limitation of this study is that, due to the expensive, time and labor intensive nature of HIEC experiments, Sirt6BAC; *Sirt6*$^{-/-}$ were unable to be included. Likewise, a HIEC mouse cohort in the HCD feeding context was also unable to be completed. However, the data gleaned from the glucose homeostasis experiments presented in chapter 3, suggest that the effects on glucose homeostasis are due to SIRT6 overexpression and not due to overexpression of the other genes present in Sirt6BAC DNA. Therefore, since enhanced insulin sensitivity can explain the phenotypes observed regarding glucose homeostasis, it is fairly reasonable to make the assumption that the effects observed in the HIEC with Sirt6BAC and wild-type mice are also due to SIRT6 overexpression and not caused by overexpression of other genes overexpressed by the Sirt6BAC DNA. Additionally, since improved insulin sensitivity was observed in Sirt6BAC mice in the chow diet context, it is very unlikely that additional derangements posed by HCD feeding would eliminate the differences observed between SIRT6BAC mice and wild-type control mice. Generally speaking, it is very common in overexpression models, that a given phenotype

will become apparent only after stressing the physiology, such as with HCD feeding. Indeed, the data presented in chapter 3 on glucose homeostasis shows that the phenotypes became more apparent in the HCD context. Therefore, if HIEC were to be performed in a HCD context, I would expect to observe even more significant differences between groups than were observed in the chow diet context.

Part of the beauty of scientific research, is that for every question answered, there are two more questions that arise. This study is no exception. Future studies into the function of SIRT6 should be aimed at answering these questions: Why might overexpression of SIRT6 elicit enhanced insulin sensitivity when insulin levels are low during periods of caloric deficit (fasting, CR) when SIRT6 levels increase? What is the intracellular mechanistic nature of the enhanced insulin-sensitivity observed in in Sirt6BAC mice? Are these intracellular mechanisms consistent within different cell-types? Are the transcriptional programs previously identified to be SIRT6-dependent consistent with ones differentially regulated in the Sirt6BAC model?

To investigate these questions, future experiments using this Sirt6BAC mouse model should include a thorough dissection of the IIS pathway. Using Western blot analyses, mice should be injected with insulin, and shortly-thereafter, various tissues should be harvested including muscle, liver and WAT and assessed via Western blot analyses for overall expression and degree of altered phosphorylation status of key enzymes in this pathway including IGF1R, InsR, IRS1/2, AKT, pERK, FOXO1, PGC-1α. Additionally, microarray studies should be conducted to elucidate the upregulated/downregulated transcripts in these mice in several conditions including basal, fasting, HCD-fed, and in response to insulin. Tissue histochemistry could also be employed to assess the degree of GLUT1 plasma membrane association following these conditions. Furthermore, this mouse model should be assessed for triglyceride accumulation and adipogenesis at advanced ages in a HCD context to determine if SIRT6 overexpression protects against obesity at advanced ages. Finally, other SIRT6 models may be needed to further advance the scientific knowledge regarding SIRT6 homeostatic function. As the data presented in this work primarily implicates the liver and skeletal muscle in the phenotypes leading to enhanced glucose homeostasis, both liver and muscle-specific SIRT6 gain-of-function models may prove useful for

nailing down these phenotypes. Lastly, chromatin immunoprecipitation sequencing (CHIP-seq) and microarray experiments could be used to isolate the differentially-regulated transcriptional programs regulated by SIRT6 in Sirt6BAC mice to determine if these support previously identified- or reveal novel transcriptional programs mediated by SIRT6 and transcription factors such as HIF-1α, RelA, c-Jun, and MYC.

FIGURES:

FIGURE 1:

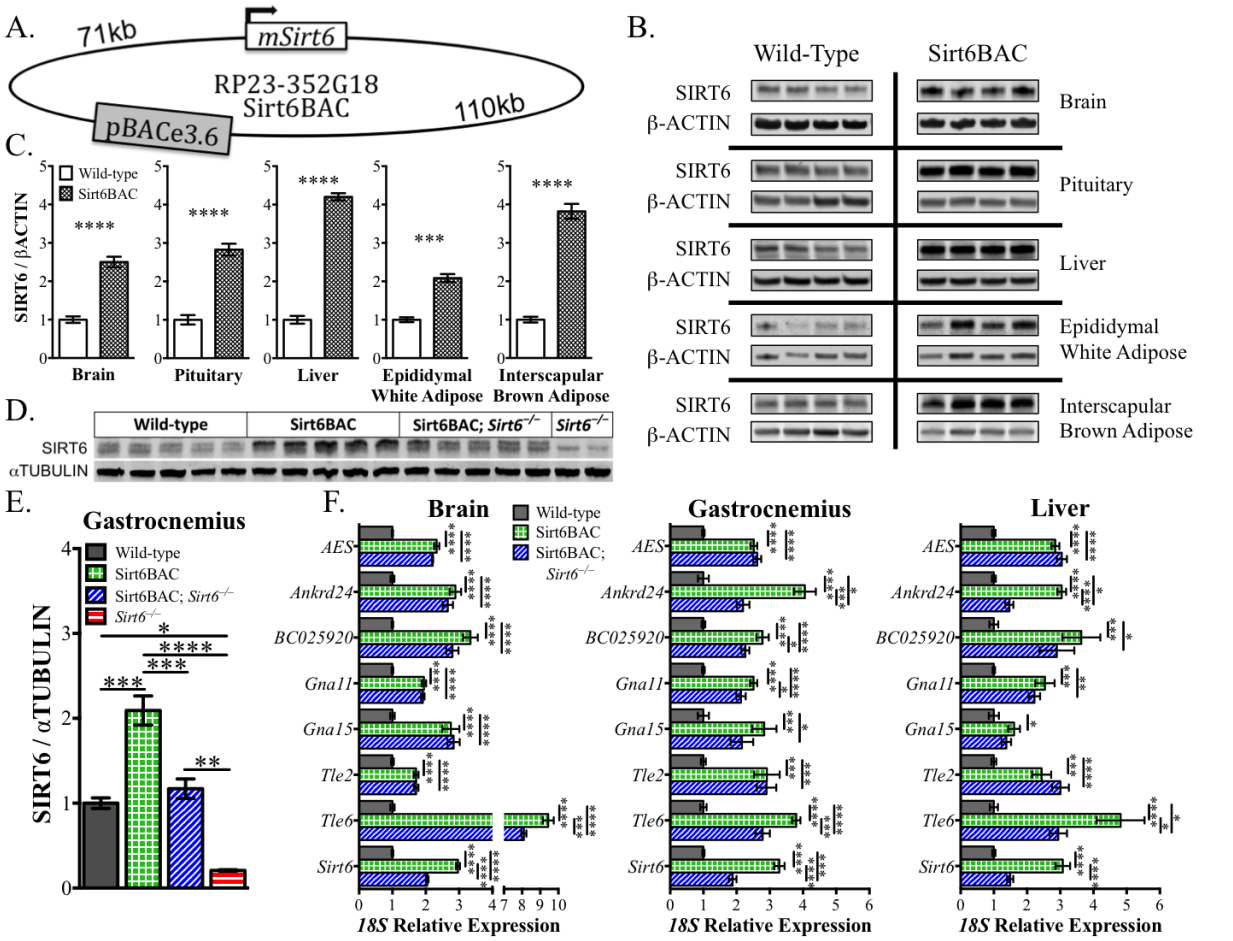

Figure 1. Sirt6BAC mice eutopically overexpress mouse SIRT6.

(A) Schematic representation of the RP23-352G18 (BACPAC Resources, Children's Hospital Oakland Research Institute) BAC DNA construct containing the mouse *Sirt6* gene used to generate Sirt6BAC mice. **(B)** Anti-SIRT6 Western blots from Sirt6BAC and wild-type mouse tissues from original founder line (pure C57Bl/6 genetic background). (Each lane represents tissue from a single mouse) **(C)** Quantification of the relative SIRT6/βACTIN expression shown in panel B (n = 4 per group). **(D)** Anti-SIRT6 Western-blot in gastrocnemius tissue from F3 C57Bl/6;129SvJ mixed genetic background (Each lane represents tissue from a single mouse). **(E)** Quantification of the relative SIRT6/αTUBULIN expression shown in panel D. **(F)** qPCR measurements of brain, gastrocnemius and liver gene transcripts present on Sirt6BAC from F3 C57Bl/6;129SvJ mixed genetic background mice (n = 6-8 per group). Values are mean ± S.E.M. Statistics were analyzed using unpaired two-tailed t-test when 2 groups were compared and one-way ANOVA with Tukey correction for multiple comparisons when 3 or more groups were compared (*p<0.05, **p<0.01, ***p<0.001, ****p<0.0001).

FIGURE 2:

A.

Genotype	n	Mendelian Ratio Observed	Mendelian Ratio Expected	Observed / Expected
Wild-type	36	0.138	0.125	110.8%
Sirt6BAC	35	0.135	0.125	107.7%
***Sirt6*$^{-/-}$**	9	0.035	0.125	27.7%
Sirt6BAC; *Sirt6*$^{-/-}$	37	0.142	0.125	113.8%

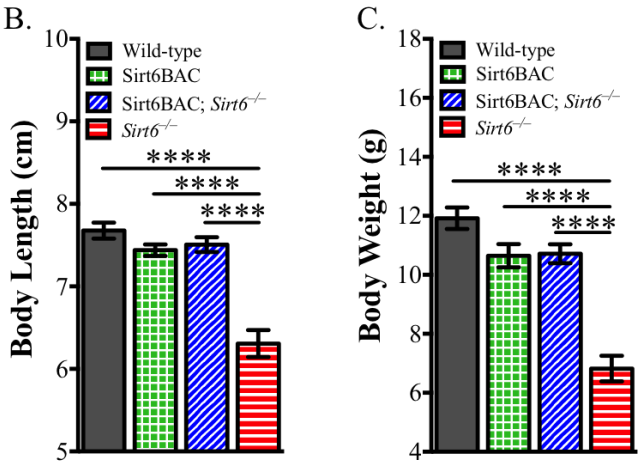

Figure 2. SIRT6 generated from Sirt6BAC is functionally competent.

(A) Viable mice per genotype observed at 4-weeks of age, shown as a percentage of the expected Mendilian ratio from F3 C57Bl/6;129SvJ inbred mixed genetic background. **(B)** Body length (n = 9-13 per group) and **(C)** body weight (n = 9-13 per group) of 3 week-old mice from F3 C57Bl/6;129SvJ mixed genetic background. Values are mean ± S.E.M. Statistics were analyzed using one-way ANOVA with Tukey correction for multiple comparisons (****$p<0.0001$).

FIGURE 3:

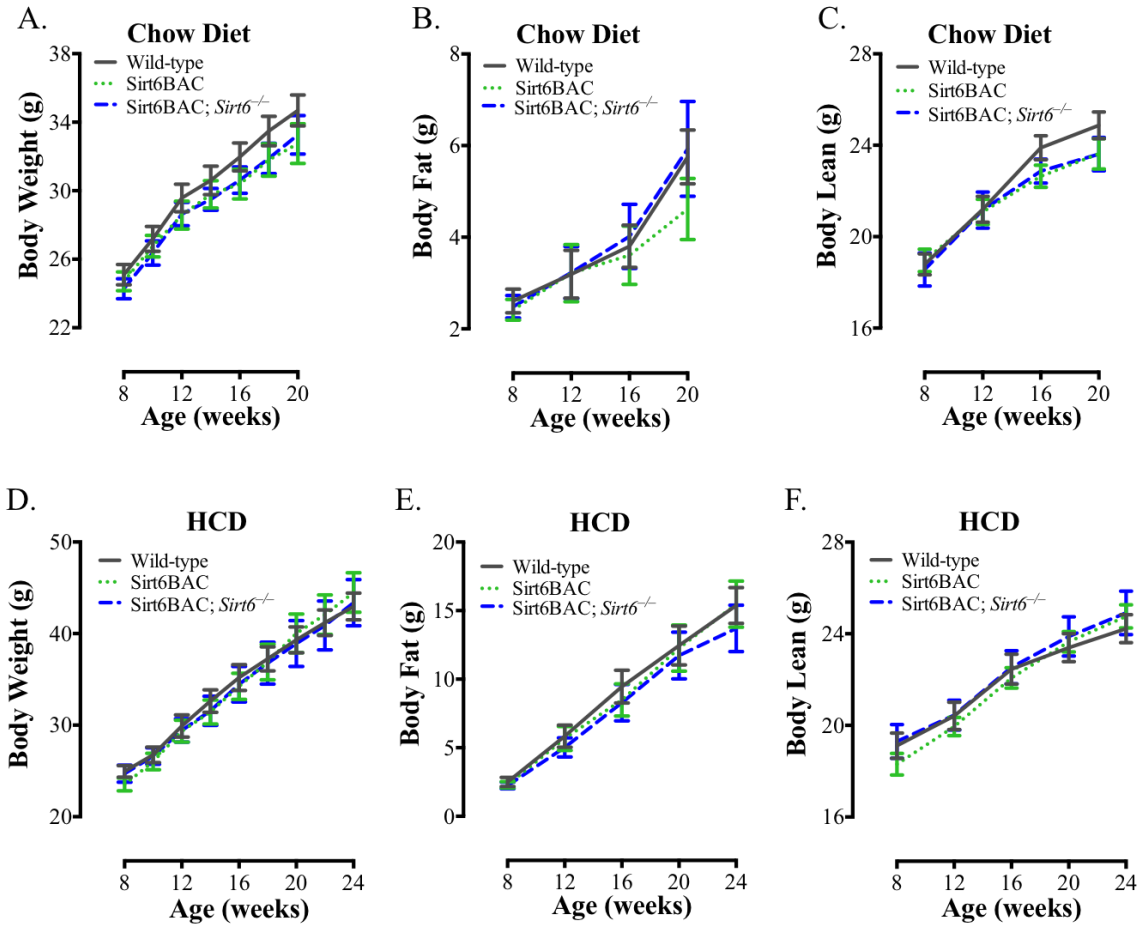

Figure 3. Sirt6BAC mice display normal body weight, fat mass and lean mass.

(A) Body weight, **(B)** body fat weight, and **(C)** body lean weight of mice in chow diet context (n = 14-21 per group). **(D)** Body weight, **(E)** body fat weight, and **(F)** body lean weight of mice in HCD context (n = 10-14 per group). Values are mean ± S.E.M. Statistics were analyzed using a repeated measures two-way ANOVA with Tukey correction for multiple comparisons.

FIGURE 4:

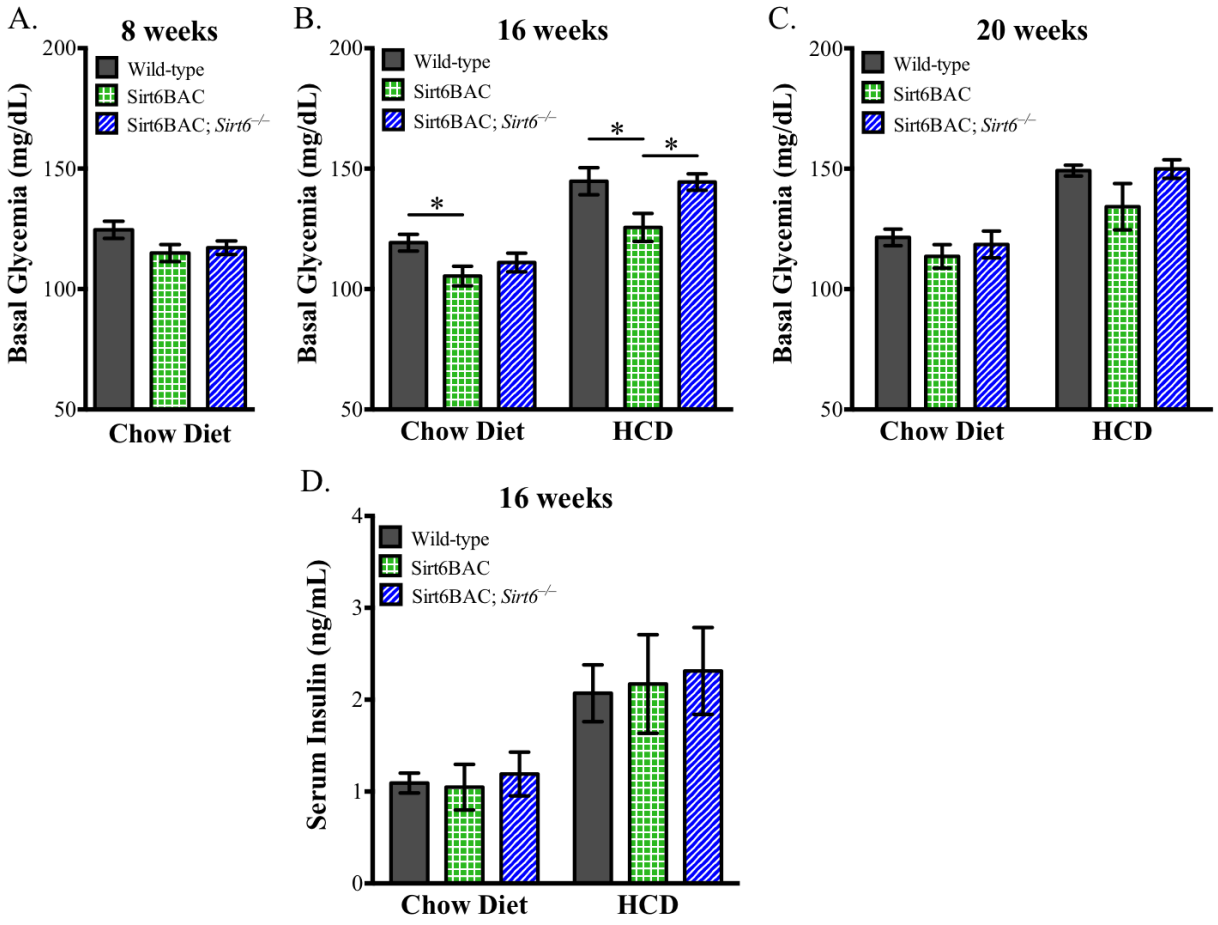

Figure 4. Sirt6BAC mice exhibit reduced glycemia, without altered insulinemia.

(A) Basal (non-postprandial) glycemia of 8 weeks old mice on chow diet (n = 19-21 per group). **(B)** Basal (non-postprandial) glycemia of 16 weeks old mice on chow diet (n = 17-24 per group) or HCD (n = 9-12 per group). **(C)** Basal (non-postprandial) glycemia of 20 weeks old mice on chow diet (n = 17-24 per group) or HCD (n = 8-10 per group). **(D)** Basal (non-postprandial) serum insulin levels of 16-weeks-old mice on chow diet (n = 9-15 per group) or HCD (n = 8-10 per group). Values are mean ± S.E.M. Statistics were analyzed using one-way ANOVA with Tukey correction for multiple comparisons (*$p<0.05$).

FIGURE 5:

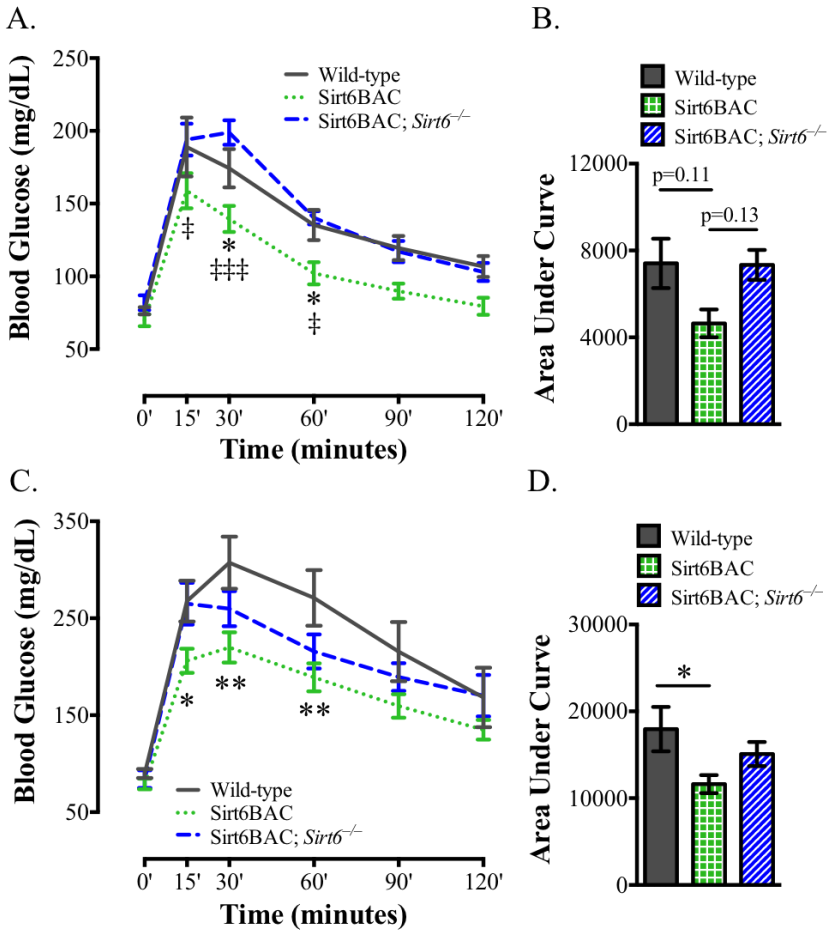

Figure 5. Sirt6BAC mice exhibit enhanced glucose tolerance.

(A) Glucose (1.5g / kg bodyweight) tolerance test and **(B)** area under curve of mice at 11-13 weeks of age in the chow diet context (n = 6-8 per group). **(C)** Glucose (1.5g / kg bodyweight) tolerance test and **(D)** area under curve of mice at 18-20 weeks of age in the HCD context (n = 5-10 per group). Values are mean ± S.E.M. Panels A&C: Statistics were analyzed using a repeated measures two-way ANOVA with Tukey correction for multiple comparisons (*p<0.05, **p<0.01 Wild-type vs. Sirt6BAC), (‡p<0.05, ‡‡‡p<0.001 Sirt6BAC vs. Sirt6BAC; *Sirt6*$^{-/-}$). Panels B&C: Statistics were analyzed using one-way ANOVA with Tukey correction for multiple comparisons (*p<0.05).

FIGURE 6:

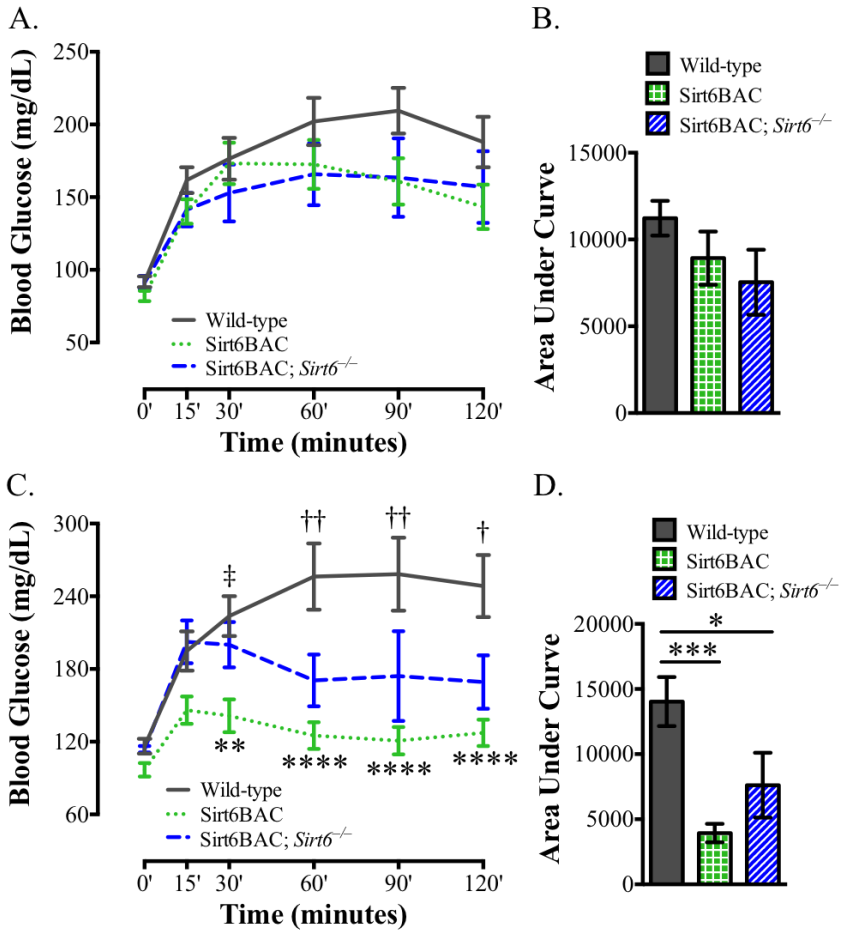

Figure 6. Sirt6BAC mice exhibit enhanced pyruvate tolerance.

(A) Pyruvate (2g / kg bodyweight) tolerance test and **(B)** area under curve of chow-diet cohort mice at 25-26 weeks of age (n = 5-8 per group). **(C)** Pyruvate (2g / kg bodyweight) tolerance test and **(D)** area under curve of HCD cohort mice at 26-28 weeks of age (n = 5-10 per group). Values are mean ± S.E.M. Panel A&C: Statistics were analyzed using a repeated measures two-way ANOVA with Tukey correction for multiple comparisons (**p<0.01, ****p<0.0001 Wild-type *vs.* Sirt6BAC), (†p<0.05, ††p<0.01 Wild-type vs. Sirt6BAC; *Sirt6*$^{-/-}$), (‡p<0.05 Sirt6BAC vs. Sirt6BAC; *Sirt6*$^{-/-}$). Panel B&D: Statistics were analyzed using one-way ANOVA with Tukey correction for multiple comparisons (*p<0.05, ***p<0.001).

FIGURE 7:

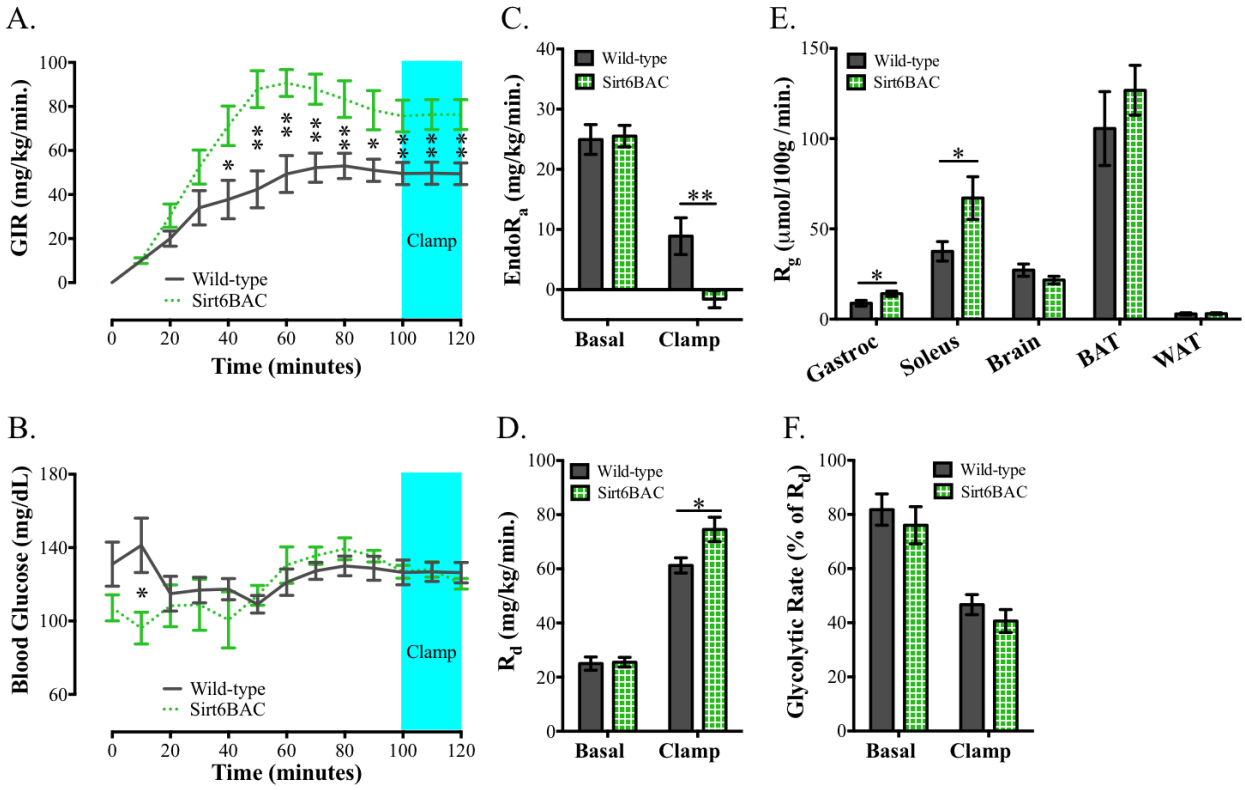

Figure 7. Sirt6BAC mice exhibit enhanced insulin sensitivity.

(A) Glucose infusion rate (GIR) (mg glucose/kg bodyweight/minute) **(B)** Blood glucose (mg/dL) **(C)** Endogenous glucose appearance ($EndoR_a$) (mg/kg bodyweight/minute) **(D)** Glucose disposal (R_d) (mg/kg bodyweight/minute) **(E)** Tissue glucose uptake (R_g) (μmol/100g tissue/minute) **(G)** Glycolytic rate (% of R_d). n = 6-8 per group. Values are mean ± S.E.M. Panels A&B: Statistics were analyzed using a repeated measures one-way ANOVA with Tukey correction for multiple comparisons (*p<0.05, **p<0.01). Panels C,D,E&F: Statistics were analyzed using unpaired two-tailed t-test (*p<0.05, **p<0.01).

Primer Tables:

Primer Table 1:

5’GACTGGGACCACACCAGAGT & 5’GTGAGAGCGGGAAGAGTACG;

5’AGGTGCCTGTGGACACTACC & 5’CAGGGGACACACTGGTTTCT;

5’CTGTCCACCTGTTGGAAGGT & 5’CTTCTGGGTCACCACAAGGT;

5’CATGAATGCTGTTTGGTTGG & 5’ATGCTGTAGGGTGGGAAGTG;

5’CCTTTGGAAAAGCAGTCAGC & 5’GAACTCCTGGCAAGTCGAAG;

5’CCACTGGGTCAGTCACACAC & 5’AGGACTCCACCTGGATTGTG.

Primer Table 2:

5’gataaactaccgcattaaagcttatcgatgataagctgtcaaacatgagaattgatccggATATATGAGTAAACTTGGTCTGAC & 5’gttaaccgggctgcatccgatgcaagtgtgtcgctgtcgacggtgaccctatagtcgaggCGGTATTTTCTCCTTACGCATC. (lowercase letters represent homologous antisense nucleotides to sequences adjacent to the loxP sequence in the RP23-352G18 BAC clone to be replaced via homologous recombination)

Primer Table 3:

5'TTGCTCTTGCGGGAAGCCCG & 5'GATACCGAGGGCGCCGTTCG (specific to the pBACe3.6 backbone sequence of RP23-352G18)

5’TTGCTGCATCAGGAGGGCGC & 5’TCCCACAATGCCCCGCTTCG (specific to the wild-type *Sirt6* allele)

BIBLIOGRAPHY

1. Bordone L et al. (2007) SIRT1 transgenic mice show phenotypes resembling calorie restriction. *Aging Cell* 6:759–767.

2. Chalkiadaki A, Guarente L (2012) Sirtuins mediate mammalian metabolic responses to nutrient availability. *Nat Rev Endocrinol* 8:287–296.

3. Mostoslavsky R et al. (2006) Genomic instability and aging-like phenotype in the absence of mammalian SIRT6. *Cell* 124:315–329.

4. Kanfi Y et al. (2010) SIRT6 protects against pathological damage caused by diet-induced obesity. *Aging Cell* 9:162–173.

5. Kanfi Y et al. (2012) The sirtuin SIRT6 regulates lifespan in male mice. *Nature* 483:218–221.

6. Grundy SMS, Brewer HBH, Cleeman JIJ, Smith SCS, Lenfant CC (2004), pp 433–438.

7. Shaw RJ et al. (2005) The kinase LKB1 mediates glucose homeostasis in liver and therapeutic effects of metformin. *Science* 310:1642–1646.

8. Zhou G et al. (2001) Role of AMP-activated protein kinase in mechanism of metformin action. *J Clin Invest* 108:1167–1174.

9. Fryer LGD, Parbu-Patel A, Carling D (2002) The Anti-diabetic drugs rosiglitazone and metformin stimulate AMP-activated protein kinase through distinct signaling pathways. *J Biol Chem* 277:25226–25232.

10. Fontana L, Klein S (2007) Aging, adiposity, and calorie restriction. *JAMA* 297:986–994.

11. Weindruch R, Sohal RS (1997) Caloric intake and aging. *The New England journal of medicine*.

12. Nisoli E et al. (2005) Calorie restriction promotes mitochondrial biogenesis by inducing the expression of eNOS. *Science* 310:314–317.

13. Civitarese AE et al. (2007) Calorie restriction increases muscle mitochondrial biogenesis in healthy humans. *PLoS Med* 4:e76.

14. Colman RJ et al. (2009) Caloric Restriction Delays Disease Onset and Mortality in Rhesus Monkeys. *Science* 325:201–204.

15. Michán S, Sinclair D (2007) Sirtuins in mammals: insights into their biological function. *Biochem J* 404:1–13.

16. Mattison JA et al. (2012) Impact of caloric restriction on health and survival in rhesus monkeys from the NIA study. *Nature* 489:318–321.

17. Weindruch R, Walford RL (1988) The retardation of aging and disease by dietary restriction.

18. Roth GS, Ingram DK, Lane MA (2001) Caloric restriction in primates and relevance to humans. *Annals of the New York Academy of Sciences* 928:305–315.

19. Wolf NS (2010) *The Comparative Biology of Aging*.

20. Tatar M et al. (2001) A mutant Drosophila insulin receptor homolog that extends life-span and impairs neuroendocrine function. *Science* 292:107–110.

21. Suh Y et al. (2008) Functionally significant insulin-like growth factor I receptor mutations in centenarians. *Proc Natl Acad Sci USA* 105:3438–3442.

22. Holzenberger M et al. (2002) IGF-1 receptor regulates lifespan and resistance to oxidative stress in mice. *Nature* 421:182–187.

23. Vitale G et al. (2012) Low circulating IGF-I bioactivity is associated with human longevity: findings in centenarians' offspring. *Aging (Albany NY)* 4:580–589.

24. Selman C et al. (2008) Evidence for lifespan extension and delayed age-related biomarkers in insulin receptor substrate 1 null mice. *FASEB J* 22:807–818.

25. Fontana L, Partridge L, Longo VD (2010) Extending healthy life span--from yeast to humans. *Science* 328:321–326.

26. Powers RW (2006) Extension of chronological life span in yeast by decreased TOR pathway signaling. *Genes & Development* 20:174–184.

27. Kapahi P et al. (2004) Regulation of Lifespan in Drosophila by Modulation of Genes in the TOR Signaling Pathway. *Current Biology* 14:885–890.

28. Bjedov I et al. (2010) Mechanisms of life span extension by rapamycin in the fruit fly Drosophila melanogaster. *Cell Metab* 11:35–46.

29. Bonawitz ND, Chatenay-Lapointe M, Pan Y (2007) Reduced TOR signaling extends chronological life span via increased respiration and upregulation of mitochondrial gene expression. *Cell*.

30. Kapahi P et al. (2010) With TOR, Less Is More: A Key Role for the Conserved Nutrient-Sensing TOR Pathway in Aging. *Cell Metab* 11:453–465.

31. Selman C et al. (2009) Ribosomal Protein S6 Kinase 1 Signaling Regulates Mammalian Life Span. *Science* 326:140–144.

32. Harrison DE et al. (2009) Rapamycin fed late in life extends lifespan in genetically heterogeneous mice. *Nature* 460:392–395.

33. Wei M et al. (2008) Life span extension by calorie restriction depends on Rim15 and transcription factors downstream of Ras/PKA, Tor, and Sch9. *PLoS Genet* 4:e13.

34. Fabrizio P, Pletcher SD, Minois N, Vaupel JW, Longo VD (2004) Chronological aging-independent replicative life span regulation by Msn2/Msn4 and Sod2 in Saccharomyces cerevisiae. *FEBS Letters* 557:136–142.

35. Cohen HY et al. (2004) Calorie restriction promotes mammalian cell survival by inducing the SIRT1 deacetylase. *Science* 305:390–392.

36. Longo VD, Kennedy BK (2006) Sirtuins in aging and age-related disease. *Cell* 126:257–268.

37. Kaeberlein M, McVey M, Guarente L (1999) The SIR2/3/4 complex and SIR2 alone promote longevity in Saccharomyces cerevisiae by two different mechanisms. *Genes & Development* 13:2570–2580.

38. Kim C et al. (2006) Comparison of body fat composition and serum adiponectin levels in diabetic obesity and non-diabetic obesity. *Obesity (Silver Spring)* 14:1164–1171.

39. Fontana L, Meyer TE, Klein S, Holloszy JO (2004) Long-term calorie restriction is highly effective in reducing the risk for atherosclerosis in humans. *Proc Natl Acad Sci USA* 101:6659–6663.

40. Lin S-J et al. (2002) Calorie restriction extends Saccharomyces cerevisiae lifespan by increasing respiration. *Nature* 418:344–348.

41. Landry J, Slama JT, Sternglanz R (2000) Role of NAD(+) in the deacetylase activity of the SIR2-like proteins. *Biochem Biophys Res Commun* 278:685–690.

42. Lin SJ, Defossez PA, Guarente L (2000) Requirement of NAD and SIR2 for life-span extension by calorie restriction in Saccharomyces cerevisiae. *Science* 289:2126–2128.

43. Guarente L, Imai S-I, Armstrong CM, Kaeberlein M (2000) Transcriptional silencing and longevity protein Sir2 is an NAD-dependent histone deacetylase. *Nature* 403:795–800.

44. Lin S-J, Ford E, Haigis M, Liszt G, Guarente L (2004) Calorie restriction extends yeast life span by lowering the level of NADH. *Genes & Development* 18:12–16.

45. Chen D et al. (2008) Tissue-specific regulation of SIRT1 by calorie restriction. *Genes & Development* 22:1753–1757.

46. Kawakami K, Nakamura A, Goto S (2012) Dietary restriction increases site-specific histone H3 acetylation in rat liver: possible modulation by sirtuins. *Biochem Biophys Res Commun* 418:836–840.

47. Flick F, Lüscher B (2012) Regulation of sirtuin function by posttranslational modifications. *Front Pharmacol* 3:29.

48. Ramadori G et al. (2008) Brain SIRT1: anatomical distribution and regulation by energy availability. *J Neurosci* 28:9989–9996.

49. Nemoto S, Fergusson MM, Finkel T (2004) Nutrient availability regulates SIRT1 through a forkhead-dependent pathway. *Science* 306:2105–2108.

50. Kanfi Y et al. (2008) Regulation of SIRT1 protein levels by nutrient availability. *FEBS Letters* 582:2417–2423.

51. Kim H-S et al. (2010) Hepatic-specific disruption of SIRT6 in mice results in fatty liver formation due to enhanced glycolysis and triglyceride synthesis. *Cell Metab* 12:224–236.

52. KANFI Y et al. (2008) Regulation of SIRT6 protein levels by nutrient availability. *FEBS Letters* 582:543–548.

53. Blander G, Guarente L (2004) The Sir2 family of protein deacetylases. *Annu Rev Biochem* 73:417–435.

54. Tanner KG, Landry J, Sternglanz R (2000).

55. Avalos JL, Bever KM, Wolberger C (2005) Mechanism of Sirtuin Inhibition by Nicotinamide: Altering the NAD+ Cosubstrate Specificity of a Sir2 Enzyme. *Molecular Cell* 17:855–868.

56. Ivy JM, Klar AJ, Hicks JB (1986) Cloning and characterization of four SIR genes of Saccharomyces cerevisiae. *Mol Cell Biol* 6:688–702.

57. Rine J, Herskowitz I (1987) Four genes responsible for a position effect on expression from HML and HMR in Saccharomyces cerevisiae. *Genetics* 116:9–22.

58. Aparicio OM, Billington BL, Gottschling DE (1991) Modifiers of position effect are shared between telomeric and silent mating-type loci in S. cerevisiae. *Cell*.

59. Smith JS, Boeke JD (1997) An unusual form of transcriptional silencing in yeast ribosomal DNA. *Genes & Development* 11:241–254.

60. Sinclair DA, Guarente L (1997) Extrachromosomal rDNA circles—a cause of aging in yeast. *Cell*.

61. Nyström T (2007) A bacterial kind of aging. *PLoS Genet* 3:e224.

62. Defossez PA et al. (1999) Elimination of replication block protein Fob1 extends the life span of yeast mother cells. *Molecular Cell* 3:447–455.

63. Boily G et al. (2008) SirT1 regulates energy metabolism and response to caloric restriction in mice. *PLoS ONE* 3:e1759.

64. Anderson RM, Bitterman KJ, Wood JG, Medvedik O, Sinclair DA (2003) Nicotinamide and PNC1 govern lifespan extension by calorie restriction in Saccharomyces cerevisiae. *Nature* 423:181–185.

65. Koubova J, Guarente L (2003) How does calorie restriction work? *Genes & Development* 17:313–321.

66. Couzin-Frankel J (2011) Aging Genes: The Sirtuin Story Unravels. *Science* 334:1194–1198.

67. Accili D, de Cabo R, Sinclair DA (2011) An unSIRTain role in longevity. *Nature Medicine* 17:1350–1351.

68. Kaeberlein M, Powers RW (2007) Sir2 and calorie restriction in yeast: a skeptical perspective. *Ageing Res Rev* 6:128–140.

69. Kaeberlein M, Kirkland KT, Fields S, Kennedy BK (2004) Sir2-Independent Life Span Extension by Calorie Restriction in Yeast. *Plos Biol* 2:e296.

70. Fabrizio P et al. (2005) Sir2 Blocks Extreme Life-Span Extension. *Cell* 123:655–667.

71. Burnett C et al. (2011) Absence of effects of Sir2 overexpression on lifespan in C. elegans and

Drosophila. *Nature* 477:482–485.

72. Vaquero A et al. (2004) Human SirT1 interacts with histone H1 and promotes formation of facultative heterochromatin. *Molecular Cell* 16:93–105.

73. Vaziri H et al. (2001) hSIR2(SIRT1) functions as an NAD-dependent p53 deacetylase. *Cell* 107:149–159.

74. Yeung F et al. (2004) Modulation of NF-kappaB-dependent transcription and cell survival by the SIRT1 deacetylase. *EMBO J* 23:2369–2380.

75. Ghosh HS, McBurney M, Robbins PD (2010) SIRT1 negatively regulates the mammalian target of rapamycin. *PLoS ONE* 5:e9199.

76. Rodgers JT et al. (2005) Nutrient control of glucose homeostasis through a complex of PGC-1α and SIRT1. *Nature* 434:113–118.

77. Purushotham A et al. (2009) Hepatocyte-specific deletion of SIRT1 alters fatty acid metabolism and results in hepatic steatosis and inflammation. *Cell Metab* 9:327–338.

78. Dominy JE, Lee Y, Gerhart-Hines Z (2010) Nutrient-dependent regulation of PGC-1α's acetylation state and metabolic function through the enzymatic activities of Sirt1/GCN5. *Biochimica et Biophysica …*.

79. Lagouge M et al. (2006) Resveratrol Improves Mitochondrial Function and Protects against Metabolic Disease by Activating SIRT1 and PGC-1α. *Cell* 127:1109–1122.

80. Frescas D, Valenti L, Accili D (2005) Nuclear trapping of the forkhead transcription factor FoxO1 via Sirt-dependent deacetylation promotes expression of glucogenetic genes. *J Biol Chem* 280:20589–20595.

81. Qiang L et al. (2012) Brown Remodeling of White Adipose Tissue by SirT1-Dependent Deacetylation of Pparγ. *Cell* 150:620–632.

82. Rodgers JT, Puigserver P (2007) Fasting-dependent glucose and lipid metabolic response through hepatic sirtuin 1. *Proc Natl Acad Sci USA* 104:12861–12866.

83. Wang R-H, Li C, Deng C-X (2010) Liver steatosis and increased ChREBP expression in mice carrying a liver specific SIRT1 null mutation under a normal feeding condition. *International Journal of Biological Sciences* 6:682–690.

84. Schug TT, Li X (2011) Sirtuin 1 in lipid metabolism and obesity. *Annals of medicine*.

85. Kemper JK, Xiao Z, Ponugoti B, Miao J, Fang S (2009) FXR acetylation is normally dynamically regulated by p300 and SIRT1 but constitutively elevated in metabolic disease states. *Cell Metab*.

86. Defour A, Dessalle K, Perez AC, Poyot T, Castells J (2012) Sirtuin 1 regulates SREBP-1c expression in a LXR-dependent manner in skeletal muscle. *PLoS ONE*.

87. Purushotham A, Xu Q, Lu J, Foley JF (2012) Hepatic deletion of SIRT1 decreases HNF1α/FXR signaling and induces formation of cholesterol gallstones in mice. *… and Cellular Biology*.

88. Wang C, Tian L, Popov VM, Pestell RG (2011) Acetylation and nuclear receptor action. *The Journal of steroid biochemistry …*.

89. Li X et al. (2007) SIRT1 deacetylates and positively regulates the nuclear receptor LXR. *Molecular Cell* 28:91–106.

90. Howitz KT et al. (2003) Small molecule activators of sirtuins extend Saccharomyces cerevisiae lifespan. *Nature* 425:191–196.

91. Wood JG et al. (2004) Sirtuin activators mimic caloric restriction and delay ageing in metazoans. *Nature* 430:686–689.

92. Baur JA (2010) Resveratrol, sirtuins, and the promise of a DR mimetic. *Mechanisms of Ageing and Development* 131:261–269.

93. Beher D et al. (2009) Resveratrol is Not a Direct Activator of SIRT1 Enzyme Activity. *Chemical Biology & Drug Design* 74:619–624.

94. Kaeberlein M et al. (2005) Substrate-specific activation of sirtuins by resveratrol. *J Biol Chem* 280:17038–17045.

95. Pacholec M et al. (2010) SRT1720, SRT2183, SRT1460, and Resveratrol Are Not Direct Activators of SIRT1. *Journal of Biological Chemistry* 285:8340–8351.

96. Park S-JS et al. (2012) Resveratrol ameliorates aging-related metabolic phenotypes by inhibiting cAMP phosphodiesterases. *Cell* 148:421–433.

97. Price NL et al. (2012) SIRT1 is required for AMPK activation and the beneficial effects of resveratrol on mitochondrial function. *Cell Metab* 15:675–690.

98. Cantó C et al. (2009) AMPK regulates energy expenditure by modulating NAD+ metabolism and SIRT1 activity. *Nature* 458:1056–1060.

99. Sun C et al. (2007) SIRT1 improves insulin sensitivity under insulin-resistant conditions by repressing PTP1B. *CMET* 6:307–319.

100. Banks AS et al. (2008) SirT1 Gain of Function Increases Energy Efficiency and Prevents Diabetes in Mice. *Cell Metab* 8:333–341.

101. Pfluger PT, Herranz D, Velasco-Miguel S, Serrano M, Tschop MH (2008) Sirt1 protects against high-fat diet-induced metabolic damage. *Proc Natl Acad Sci USA* 105:9793–9798.

102. Ramadori G et al. (2011) SIRT1 deacetylase in SF1 neurons protects against metabolic imbalance. *Cell Metab* 14:301–312.

103. Ramadori G et al. (2009) Central Administration of Resveratrol Improves Diet-Induced Diabetes. *Endocrinology* 150:5326–5333.

104. Baur JA et al. (2006) Resveratrol improves health and survival of mice on a high-calorie diet. *Nature* 444:337–342.

105. Milne JC et al. (2007) Small molecule activators of SIRT1 as therapeutics for the treatment of

type 2 diabetes. *Nature* 450:712–716.

106. Michishita E et al. (2008) SIRT6 is a histone H3 lysine 9 deacetylase that modulates telomeric chromatin. *Nature* 452:492–496.

107. Michishita E et al. (2009) Cell cycle-dependent deacetylation of telomeric histone H3 lysine K56 by human SIRT6. *Cell Cycle* 8:2664–2666.

108. Liszt G, Ford E, Kurtev M, Guarente L (2005) Mouse Sir2 homolog SIRT6 is a nuclear ADP-ribosyltransferase. *J Biol Chem* 280:21313–21320.

109. McCord RA et al. (2009) SIRT6 stabilizes DNA-dependent protein kinase at chromatin for DNA double-strand break repair. *Aging (Albany NY)* 1:109–121.

110. Kaidi A, Weinert BT, Choudhary C, Jackson SP (2010) Human SIRT6 promotes DNA end resection through CtIP deacetylation. *Science* 329:1348–1353.

111. Mao Z et al. (2011) SIRT6 promotes DNA repair under stress by activating PARP1. *Science* 332:1443–1446.

112. Mao Z et al. (2012) Sirtuin 6 (SIRT6) rescues the decline of homologous recombination repair during replicative senescence. *Proc Natl Acad Sci USA* 109:11800–11805.

113. Tian B, Brasier AR (2003) Identification of a nuclear factor kappa B-dependent gene network. *Recent Prog Horm Res* 58:95–130.

114. Brasier AR (2006) The NF-κB regulatory network. *Cardiovascular toxicology*.

115. Gilmore TD (2006) Introduction to NF-κB: players, pathways, perspectives. *Oncogene*.

116. Perkins ND (2007) Integrating cell-signalling pathways with NF-kappaB and IKK function. *Nat Rev Mol Cell Biol* 8:49–62.

117. Chandel NS, Trzyna WC, McClintock DS, Schumacker PT (2000) Role of oxidants in NF-kappa B activation and TNF-alpha gene transcription induced by hypoxia and endotoxin. *J Immunol* 165:1013–1021.

118. Jacobs MD, Harrison SC (1998) Structure of an IkappaBalpha/NF-kappaB complex. *Cell* 95:749–758.

119. Kawahara TLA et al. (2009) SIRT6 links histone H3 lysine 9 deacetylation to NF-kappaB-dependent gene expression and organismal life span. *Cell* 136:62–74.

120. Schwer B et al. (2010) Neural sirtuin 6 (Sirt6) ablation attenuates somatic growth and causes obesity. *Proc Natl Acad Sci USA* 107:21790–21794.

121. Cohen DE, Supinski AM, Bonkowski MS, Donmez G, Guarente LP (2009) Neuronal SIRT1 regulates endocrine and behavioral responses to calorie restriction. *Genes & Development* 23:2812–2817.

122. Ramadori G et al. (2010) SIRT1 deacetylase in POMC neurons is required for homeostatic defenses against diet-induced obesity. *Cell Metab* 12:78–87.

123. Sundaresan NR et al. (2012) The sirtuin SIRT6 blocks IGF-Akt signaling and development of cardiac hypertrophy by targeting c-Jun. *Nature Medicine* 18:1643–1650.

124. Sansone L et al. (2013) SIRT1 silencing confers neuroprotection through IGF-1 pathway activation. *J Cell Physiol* 228:1754–1761.

125. Zhong L et al. (2010) The histone deacetylase Sirt6 regulates glucose homeostasis via Hif1alpha. *Cell* 140:280–293.

126. Lum JJ et al. (2007) The transcription factor HIF-1alpha plays a critical role in the growth factor-dependent regulation of both aerobic and anaerobic glycolysis. *Genes & Development* 21:1037–1049.

127. Seagroves TN et al. (2001) Transcription factor HIF-1 is a necessary mediator of the pasteur effect in mammalian cells. *Mol Cell Biol* 21:3436–3444.

128. Aragonés J, Fraisl P, Baes M, Carmeliet P (2009) Oxygen sensors at the crossroad of metabolism. *Cell Metab* 9:11–22.

129. Vander Heiden MG, Cantley LC, Thompson CB (2009) Understanding the Warburg effect: the metabolic requirements of cell proliferation. *Science* 324:1029–1033.

130. Hu C-J et al. (2006) Differential regulation of the transcriptional activities of hypoxia-inducible factor 1 alpha (HIF-1alpha) and HIF-2alpha in stem cells. *Mol Cell Biol* 26:3514–3526.

131. Kim J, Tchernyshyov I, Semenza GL, Dang CV (2006) HIF-1-mediated expression of pyruvate dehydrogenase kinase: a metabolic switch required for cellular adaptation to hypoxia. *Cell Metab*.

132. Papandreou I, Cairns RA, Fontana L, Lim AL, Denko NC (2006) HIF-1 mediates adaptation to hypoxia by actively downregulating mitochondrial oxygen consumption. *CMET* 3:187–197.

133. Xiao C et al. (2010) SIRT6 Deficiency Results in Severe Hypoglycemia by Enhancing Both Basal and Insulin-stimulated Glucose Uptake in Mice. *Journal of Biological Chemistry* 285:36776–36784.

134. Warburg O (1956) On the origin of cancer cells. *Science*.

135. Sebastian C et al. (2012) The histone deacetylase SIRT6 is a tumor suppressor that controls cancer metabolism. *Cell* 151:1185–1199.

136. van Riggelen J, Yetil A, Felsher DW (2010) MYC as a regulator of ribosome biogenesis and protein synthesis. *Nat Rev Cancer* 10:301–309.

137. Yang SJ et al. (2011) Activation of peroxisome proliferator-activated receptor gamma by rosiglitazone increases sirt6 expression and ameliorates hepatic steatosis in rats. *PLoS ONE* 6:e17057.

138. Nemoto S, Fergusson MM, Finkel T (2005) SIRT1 functionally interacts with the metabolic regulator and transcriptional coactivator PGC-1{alpha}. *J Biol Chem* 280:16456–16460.

139. Coste A et al. (2008) The genetic ablation of SRC-3 protects against obesity and improves

insulin sensitivity by reducing the acetylation of PGC-1{alpha}. *Proc Natl Acad Sci USA* 105:17187–17192.

140. Dominy JE Jr. et al. (2012) The Deacetylase Sirt6 Activates the Acetyltransferase GCN5 and Suppresses Hepatic Gluconeogenesis. *Cell*.

141. Liang Y, Cincotta AH (2001) Increased responsiveness to the hyperglycemic, hyperglucagonemic and hyperinsulinemic effects of circulating norepinephrine in ob/ob mice. *Int J Obes Relat Metab Disord* 25:698–704.

142. Zhong L, Mostoslavsky R (2010) SIRT6: a master epigenetic gatekeeper of glucose metabolism. *Transcription* 1:17–21.

143. Quitschke WW, Lin ZY, DePonti-Zilli L, Paterson BM (1989) The beta actin promoter. High levels of transcription depend upon a CCAAT binding factor. *J Biol Chem* 264:9539–9546.

144. Alexopoulou A, Couchman J, Whiteford J (2008) … /chicken β actin (CAG) promoter can be used to drive transgene expression during the differentiation of murine embryonic stem cells into vascular progenitors. *BMC cell biology*.

145. Balthasar N et al. (2004) Leptin Receptor Signaling in POMC Neurons Is Required for Normal Body Weight Homeostasis. *Neuron* 42:983–991.

146. Lee EC et al. (2001) A highly efficient Escherichia coli-based chromosome engineering system adapted for recombinogenic targeting and subcloning of BAC DNA. *Genomics* 73:56–65.

147. Hogan B, Costantini F, Lacy E (1986) Manipulating the mouse embryo: a laboratory manual.

148. Bookout AL, Cummins CL, Mangelsdorf DJ, Pesola JM, Kramer MF (2006) High-throughput real-time quantitative reverse transcription PCR. *Curr Protoc Mol Biol* Chapter 15:Unit 15.8.

149. Miyake K et al. (2002) Hyperinsulinemia, glucose intolerance, and dyslipidemia induced by acute inhibition of phosphoinositide 3-kinase signaling in the liver. *J Clin Invest* 110:1483–1491.

150. Lin J et al. (2004) Defects in adaptive energy metabolism with CNS-linked hyperactivity in PGC-1alpha null mice. *Cell* 119:121–135.

151. DeFronzo RA, Tobin JD, Andres R (1979) Glucose clamp technique: a method for quantifying insulin secretion and resistance. *Am J Physiol* 237:E214–23.

152. Muniyappa R, Lee S, Chen H, Quon MJ (2008) Current approaches for assessing insulin sensitivity and resistance in vivo: advantages, limitations, and appropriate usage. *Am J Physiol Endocrinol Metab* 294:E15–26.

153. Ayala JE et al. (2011) Hyperinsulinemic-euglycemic clamps in conscious, unrestrained mice. *J Vis Exp*.

154. Lombard DB, Schwer B, Alt FW, Mostoslavsky R (2008) SIRT6 in DNA repair, metabolism and ageing. *Journal of Internal Medicine* 263:128–141. Available at: http://onlinelibrary.wiley.com/doi/10.1111/j.1365-2796.2007.01902.x/full.